

Comparison of market designs ensuring network integrity in low voltage distribution systems with high DER penetration

Gorrasi, Chiara; Bruninx, Kenneth; Delarue, Erik

DOI

[10.1016/j.apenergy.2024.123804](https://doi.org/10.1016/j.apenergy.2024.123804)

Publication date

2024

Document Version

Final published version

Published in

Applied Energy

Citation (APA)

Gorrasi, C., Bruninx, K., & Delarue, E. (2024). Comparison of market designs ensuring network integrity in low voltage distribution systems with high DER penetration. *Applied Energy*, 372, Article 123804. <https://doi.org/10.1016/j.apenergy.2024.123804>

Important note

To cite this publication, please use the final published version (if applicable). Please check the document version above.

Copyright

Other than for strictly personal use, it is not permitted to download, forward or distribute the text or part of it, without the consent of the author(s) and/or copyright holder(s), unless the work is under an open content license such as Creative Commons.

Takedown policy

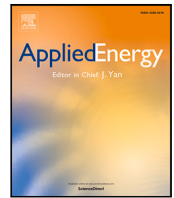
Please contact us and provide details if you believe this document breaches copyrights. We will remove access to the work immediately and investigate your claim.

Green Open Access added to TU Delft Institutional Repository

'You share, we take care!' - Taverne project

<https://www.openaccess.nl/en/you-share-we-take-care>

Otherwise as indicated in the copyright section: the publisher is the copyright holder of this work and the author uses the Dutch legislation to make this work public.



Comparison of market designs ensuring network integrity in low voltage distribution systems with high DER penetration

Chiara Gorrasi^{a,b}, Kenneth Bruninx^c, Erik Delarue^{a,b,*}

^a Applied Mechanics and Energy Conversion (TME), Department of Mechanical Engineering, KU Leuven, Celestijnenlaan 300, Leuven 3001, Belgium

^b EnergyVille, Thor Park 8310, Genk 3600, Belgium

^c Faculty of Technology, Policy and Management, TU Delft, Jaffalaan 5, Delft 2628 BX, Netherlands

ARTICLE INFO

Keywords:

Prosumer
Distribution networks
Dynamic operating envelope (DOE)
Distribution locational marginal pricing (DLMP)

ABSTRACT

This study delves into the interplay of residential electricity customers in low voltage distribution systems (LVDS) with market designs that manage local grid constraints. Within this context, residential electricity customers are self-interested agents, exposed to real-time pricing, that can invest in distributed energy resources (DER) and participate in wholesale energy as well as ancillary service market. The study specifically evaluates the trade-off between market design complexity and economic efficiency by examining market designs that employ Static Limits (SLs), Dynamic Operating Envelopes (DOEs), and Distribution Locational Marginal Pricing (DLMP) to ensure network integrity. Using a long-run equilibrium problem the study comprises both operational and investment perspective, considering feedbacks between distribution and higher voltage levels. The analysis reveals three key insights. Firstly, simpler market designs, namely SL-based and DOE-based designs, can approximate the economic efficiency of DLMP-based design, contingent on the network's characteristics. Effective in networks comprised of shorter feeders and larger consumers, the efficacy of simpler designs in approximating DLMP-based design diminishes in networks comprising longer feeders and numerous small consumers. Secondly, consumer preferences play a crucial role in DOE-based design, with consumers having a high willingness-to-pay (WTP) for grid capacity influencing economic efficiency. Thirdly, despite differences in distribution, energy, and DER investment costs, for the majority of consumers, total costs remain comparable across the three designs.

1. Introduction

1.1. Motivation and related work

Favourable regulatory frameworks, cost declines and technological advancements have rendered distributed energy resources (DERs) increasingly accessible. This has enabled a paradigm shift in the generation and consumption of power, giving rise to a growing number of prosumers: residential electricity customers actively involved in the production and/or storage of electricity. Aligning DERs with the wholesale market can help unlock their full potential, fostering a more resilient, sustainable, and consumer-centric energy system. However, amidst market integration efforts, the interaction of self-interested agents with low voltage distribution systems (LVDS) introduces a nuanced challenge. Uncontrolled, this interaction holds the potential to violate physical as well as operational network limits at the local level, underscoring the imperative for mechanisms that can effectively

manage local grid constraints. To fully harness the benefits of DERs, it is essential not only to integrate them into the wholesale market but also to judiciously manage their interactions at the local level, ensuring the stability and reliability of the network infrastructure.

In safeguarding the integrity of the network, it is crucial that the mechanisms devised for this purpose remain technology-neutral and forward-looking [1]. Central to this is the recognition of consumer autonomy. While granting prosumers the flexibility to manage their assets according to their preferences and circumstances, network integrity can be safeguarded through two mechanisms: (i) influencing the behaviours of decision-makers with appropriate market signals, aligning DER operation with system needs or (ii) directly limiting the operational decisions consumers can make, e.g., by defining export/import limits.¹

Within the second group, a straightforward approach is the implementation of static limits (SLs). Typically, with a primary focus on restricting exports, these limits have been mandated by Distribution

* Corresponding author at: Applied Mechanics and Energy Conversion (TME), Department of Mechanical Engineering, KU Leuven, Celestijnenlaan 300, Leuven 3001, Belgium.

E-mail addresses: chiara.gorrasi@kuleuven.be (C. Gorrasi), k.bruninx@tudelft.nl (K. Bruninx), erik.delarue@kuleuven.be (E. Delarue).

¹ In this work import/export refers to agent's offtake/injection.

Nomenclature

Sets

\mathcal{G}	Set of conventional generators, indexed by g .
\mathcal{J}	Set of consumers, indexed by j .
\mathcal{L}	Set of network branches, indexed by l .
\mathcal{N}	Set of network nodes, indexed by n .
\mathcal{T}	Set of time steps, indexed by t .
Φ	Set of phases, indexed by ϕ .

Parameters

Ω	Network capacity granted by network-aware market operator, kW.
N^ϕ	Number of residential consumers in network connected to phase ϕ .
$AF_{t,o}^{PV}$	Availability factor of solar PV at time step t for orientation o .
AF_t^W	Availability factor of wind at time step t .
$P_{j,t,\phi}$	Active power demand of consumer j at time step t on phase ϕ , kWh.
$Q_{j,t,\phi}$	Reactive power demand of consumer j at time step t on phase ϕ , kVAR.
η^{ch}	Charging efficiency of battery storage, %.
η^{dc}	Discharging efficiency of battery storage, %.
$P_{t,\phi}^{HV}$	Active power demand occurring at higher voltage at time step t on phase ϕ , MWh.
$Q_{t,\phi}^{HV}$	Reactive power demand occurring at higher voltage at time step t on phase ϕ , MVAR.
IC_j^S	Perceived, annualized investment cost of battery storage for consumer j , €/kWh.y.
IC_j^{Si}	Perceived, annualized investment cost of battery inverter for consumer j , €/kW.y.
IC_g^C	Annualized investment cost of conventional generator g , €/MW.y.
IC_j^{PV}	Perceived, annualized investment cost of solar PV panel for consumer j , €/kW.y.
IC_j^{PVi}	Perceived, annualized investment cost of solar PV inverter for consumer j , €/kW.y.
IC^W	Annualized investment cost of wind farm, €/MW.y.
$P_{t,n,\phi}^{LV}$	Active power demand occurring at low voltage at time step t on node n on phase ϕ , kWh.
$Q_{t,n,\phi}^{LV}$	Reactive power demand occurring at low voltage at time step t on node n on phase ϕ , kVAR.
CAP_j^S	Maximum battery storage capacity that can be installed by consumer j , kWh.
CAP_j^{PV}	Maximum solar PV panel capacity that can be installed by consumer j , kW.
κ	Power factor.
SOC^E	State of charge for battery storage at end and beginning of each day, %.
\overline{SOC}	Maximum state of charge for battery storage, %.
\underline{SOC}	Minimum state of charge for battery storage, %.
VC_g^P	Variable cost of active power production of conventional generator g , €/MWh.
VC_g^Q	Variable cost of reactive power production of conventional generator g , €/MVAR.

Primal variables

$e_{j,t}$	Energy content of battery storage of consumer j at time step t , kWh.
cap_j^S	Battery storage capacity installed by consumer j , kWh.
cap_j^{Si}	Battery inverter capacity installed by consumer j , kW.
cap_g^C	Installed capacity of conventional generator g , MW.
cap_j^{PV}	Solar PV panel capacity installed by consumer j , kW.
cap_j^{PVi}	Solar PV inverter capacity installed by consumer j , kW.
cap^W	Installed capacity of wind farm, MW.
$ch_{j,t}$	Energy charged to battery storage by consumer j at time step t , kWh.
$dc_{j,t}$	Energy discharged from battery storage by consumer j at time step t , kWh.
$cap_{j,t,\phi}^{DOE}$	Capacity of dynamic operating envelope of consumer j at time step t on phase ϕ , kW.
$ps_{j,t}$	Active power exchange of battery storage of consumer j at time step t , kWh.
$pi_{j,t,\phi}$	Active power grid import/export of consumer j at time step t on phase ϕ , kWh.
$pc_{g,t,\phi}$	Active power generation of conventional generator g at time step t on phase ϕ , MWh.
$ps_{j,t}$	Active power generation from solar PV panel of consumer j at time step t , kW.
$pw_{t,\phi}$	Active power generation of wind farm at time step t on phase ϕ , MWh.
$qi_{j,t,\phi}$	Reactive power grid import/export of consumer j at time step t on phase ϕ , kVAR.
$qc_{g,t,\phi}$	Reactive power generation of conventional generator g at time step t on phase ϕ , MVAR.
$qs_{j,t}$	Reactive power generation from solar PV inverter of consumer j at time step t , kW.

Dual variables

$\mu_{t,\phi}$	Network capacity price at time step t on phase ϕ , €/kW.
$\lambda_{t,n,\phi}^P$	Active power price at time step t on node n and phase ϕ , €/MWh.
$\lambda_{t,n,\phi}^Q$	Reactive power price at time step t on node n and phase ϕ , €/MVAR.

As highlighted by Neetzow et al. [2], the advent of storage, or electric vehicles (EVs), can contribute to both import and export stresses if no preventive mechanisms are in place. While most study the enforcement of SLs as a percentage of installed solar PV capacity [2–4], few explore the more technology-neutral approach of enforcing SLs at customer connection points.

One example would be the work of Azim et al. [5], which, from a purely operational perspective, disregarding branch rating limits, investigates the impact of a non-optimally set, 5 kW export limit within a P2P market in a real LV distribution network. This study reflects common practice where region-wide static limits are imposed on customer connections. Disregarding factors like unbalanced generation and customer load variation, these limits are identical for all consumers in the network, as exemplified by Energex's 5 kW export and 10 kW import limits in South East Queensland [6]. While the SL approach minimizes communication requirements and is easy for consumers to interpret, it has drawbacks, such as being overly conservative and leading to the underutilization of DERs [7]. Moreover, these static

System Operators (DSOs) in response to high solar PV penetration, aiming to reduce overvoltage and line congestion. Few currently recognize the importance of integrating export policies with import ones.

limits, derived from worst-case scenarios, may hinder the full capacity utilization of the network [8].

In addressing the limitations of static limits, the concept of Dynamic Operating Envelopes (DOEs) has garnered increased attention in recent years. A DOE can be defined as a time-varying principled allocation of available hosting capacity [9]. When applied to customer connection points, DOEs constrain the total behind-the-meter power flows, defining export and import limits that vary over time. Literature comparing SLs and DOEs has underscored the advantages of adopting the more dynamic approach [8,10–15]. The static limits employed in these studies mirror those used in real-life in certain jurisdictions, lacking optimality and assurance of network integrity [8]. Moreover, only [8] looks at the comparison between DOEs and SLs, both export and import. With the exception of [15] which considers investments in DER, the remaining studies focus on an operational perspective. In all studies, prices are exogenous to the models, disregarding how the system may adapt due to decisions made at distribution level. By not considering the most ample static limit that ensures network-feasible consumer decisions, the main conclusion is then that DOEs, unlike SLs ensure network integrity and enable more efficient utilization of network hosting capacity, with higher penetration of distributed generation. Additionally, [8,10,12–14] neglect the reactive power flexibility that can be provided by smart inverters to potentially enable greater active power export [11].

DOEs introduce complexity to the system compared to SLs, requiring more active management. Their calculation as well as communication may be a non-trivial multi-period problem that need be accurate and scalable for distribution systems with many nodes [16]. Various methods exist for DOE calculation. Examples include the use of distribution system state estimation for capacity-constrained optimization [17], decentralized frameworks using voltage measurements and forecasts [18] and linearized unbalanced three-phase optimal power flow models [19]. Additionally, several ways of allocating DOEs exist, favouring technical performance, fairness or consumer preferences. Studies [13,14] involve the use of an optimal allocation algorithm which maximizes how much capacity can be allocated to connection-points as a whole. Fairness-oriented methods, demonstrated in [10,12,16,20], unlike technical methods, avoid large discrepancies in DOE size between customers.² Alternatively, the preference-based approaches present in literature, explicitly consider consumer/aggregator preferences through negotiation of DOEs with DSOs, as presented in [8,21]. For example, in [8], although neglecting the network's branch rating constraints in their sequential approach, a DER merit order is created, where desired bids and DOEs are communicated to the DSO who then allocates greater grid capacity to those bids that will be more competitive in wholesale market. Consumer preferences can also be considered implicitly through pricing of network capacity, thereby preserving greater privacy [22,23]. Importantly, pricing network capacity not only ensures fairer cost allocation, wherein consumers with higher demands during peak times pay more, aligning with the actual costs of providing necessary capacity, but also establishes a market-driven mechanism for the optimal utilization of the electrical grid. This method, along with others considering consumer preferences, is the most economically efficient strategy within the current discourse on DOE allocation, falling at the cusp between approaches (i) influencing the behaviours of decision-makers with market signals and (ii) limiting the operational decisions consumers can make.

Exemplifying the approach of influencing decision makers with appropriate market signals, distribution locational marginal prices (DLMPs) have been labelled as the 'gold standard' in efficient short-run signals [24], yielding greatest economic efficiency and optimal network use. In theory, DLMPs guarantee maximum system social

surplus as they reflect the true value of an additional unit of consumption/generation at a specific location (node) in the network, motivating system-optimal operational and investment decisions [25, 26]. A plethora of studies have shown how DLMPs can be used to manage network constraints and indicate where prospective DER ought to connect as well as how they should be sized [27–31]. A typical assumption in studies focusing on nodal pricing for the distribution level is that the wholesale electricity price set at the slack node is exogenous to the model. There is no feedback between actions at the distribution level and those at higher voltage levels, nor any consideration of how they may influence overall price formation.

It is crucial to recognize that the accuracy of a DLMP and its components (energy price, congestion price, voltage support price and loss price) are intrinsically linked to the fidelity of the underlying power flow model, involving a delicate balance between computational efficiency and precision in representing the complexities of the power network. To overcome the computational complexity and challenges of deriving meaningful prices, brought by the non-convexities of alternating current optimal power flow (ACOPF), several studies, including ours, have proposed to obtain DLMPs for congestion management via linear approximations [32–34]. Nonetheless, the implementation of DLMPs in real-life introduces significant complexities. Advanced communication and control infrastructure for real-time data exchange and price signalling are required. Numerous distribution system nodes make the operationalization of DLMPs highly resource-intensive and limited data availability can make it challenging to calculate accurate prices. Moreover, highly active management of the network implies deeper ramifications on current DSO operation and planning practices [35], requiring new regulatory and market structures. From a consumer perspective, correctly interpreting and responding to rapidly changing prices may be difficult, especially if unequipped with smart appliances.

Overall, the literature recognizes static limits, dynamic operating envelopes and distribution locational marginal pricing as non-prescriptive means of ensuring network integrity within a context of DER market participation [1,12]. However, the literature lacks a comprehensive study that recognizes the difference in complexity of the three approaches and quantifies the trade-off in gains in economic efficiency that can occur between the three. Such an assessment is crucial as it provides essential information for stakeholders to evaluate whether the derived economic benefits justify the entailed complexity, thereby guiding informed decision-making in the design and operation of distribution-level energy markets. In our study, this comparison is performed considering the impact on both operational and investment decisions. This expands upon existing literature, which within the realm of studies on SLs and DOEs, largely focuses on the operational perspective, assessing how such mechanisms influence grid reliability [11, 12,21,36]. Considering both investment and operational perspectives is crucial because it allows for a comprehensive understanding of how market structures impact not only day-to-day operations but also long-term infrastructure planning. Additionally, while the transmission level is often treated as static in existing literature, e.g. [8,15,28,31], we explore the feedback loops between transmission and distribution level agents. This consideration allows for mutual influence between decisions made at either level, impacting both each other and price formation. This approach is crucial as it can dampen differences in economic efficiency between market designs by enabling the entire system to adapt in response to changing distribution level market designs and resulting consumers' decisions. Instead of emulating limits used in real-life, as done [8,10–15], the comparison is performed considering the maximal permissible capacity for both SLs and DOEs in order to have a fair comparison in terms of cost efficiency. Additionally, a high level of technical detail is included, such as inverter reactive power, phase imbalance, branch rating limits, voltage bounds, and losses. This is essential because it has been shown that the maximum export values depend significantly on the sets of network limits represented [37] and that inverter reactive power capabilities can help amplify exports [11].

² This is in contrast to technical methodologies wherein some connection points, particularly those farthest from the substation, can end up with no network capacity.

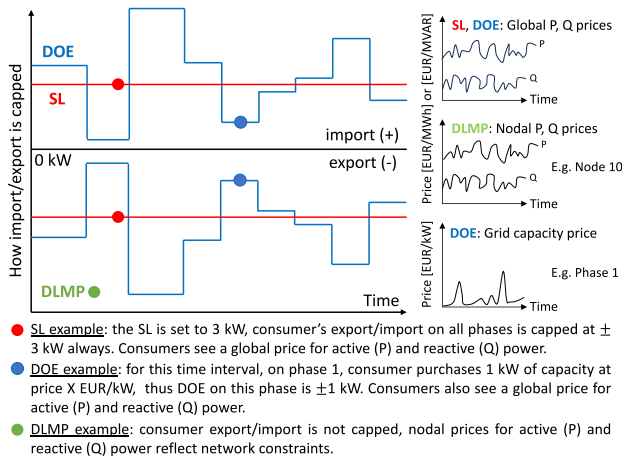


Fig. 1. Network limitations and prices as seen by a consumer at node 10, phase 1, under SL, DOE and DLMP based designs.

1.2. Contributions

This paper fills the research gap described above by determining the extent of cost efficiency gained by a DLMP-based market design in comparison to the simpler alternatives. In our SL-based design, consumers are subject to the most ample, symmetrical export and import limits that ensure network integrity. These limits are the same for all consumers, across all phases and do not change over time. In our DOE-based design, consumers bid, on an hourly basis, for per-phase network capacity. The network operator assigns network capacity based on their willingness to pay in a pay-as-cleared auction with an hourly and per-phase resolution, defining their operating envelope, *i.e.* how much they may import as well as export on each phase. A maximal aggregate amount of network capacity is made available per-phase, while ensuring a network-admissible solution. In DLMP-based design, the operational constraints of the network are embedded in the market clearing problem via linear power flow constraints. The resulting price signal directly reflects the network's status to consumers. A schematic overview of the network limitations and prices observed by a consumer under SL, DOE and DLMP concepts, are shown in Fig. 1, with a more detailed example present in Section 6.1. We construct a model that captures the long-run equilibrium between suppliers and consumers within a wholesale electricity market in which residential consumers may participate freely. Based on this, the main contributions of this paper are:

- Guidance on market design trade-offs:** We provide critical guidance to researchers, DSOs, policymakers, and regulators on balancing the complexity in different market designs required to ensure network integrity and potential gains in cost-efficiency. This is the first study to evaluate the performance of SLs, DOEs, and DLMPs, integrating both operational and investment decisions of agents at both distribution and higher voltage levels. This study illustrates how market design affects both daily operations and long-term investment strategies.
- Incorporation of feedback between voltage levels:** Our model uniquely allows for feedback between distribution and higher voltage levels. By integrating this feedback, and not taking the higher voltage levels as static, we demonstrate how transmission-level decisions can adjust to those made at the distribution level, leading to a more accurate assessment of the efficiency differences between market designs.
- Extensive comparative assessment:** We implement the proposed market designs across 14 non-synthetic, three-phase, unbalanced European LVDS, with 10 distinct consumer placements

per network, resulting in 140 cases per market design. This approach addresses the impact of varied DER deployment scenarios on market outcomes and investment decisions. Additionally, we consider real and reactive power, losses, voltage, and branch rating constraints to emulate real-world network bottlenecks, and include a reactive power market to leverage the flexibility of prosumers with smart inverters.

- Use of maximal network permissible capacity:** Our study guarantees the best-case performance of each market design by providing the maximal, network-admissible grid capacity in each case. This comprehensive approach ensures that we understand how close simpler designs can get to the efficiency of DLMP-based designs when applied effectively.

Results show that (1) SL-based and DOE-based design can approximate the economic efficiency of DLMP-based designs to within 1% when applied to networks comprising shorter, more densely populated feeders, (2) the economic efficiency of DOE-based design hinges significantly on where consumers with high willingness to pay (WTP) for grid capacity are located and (3) the total cost seen by consumers is comparable across the three market designs.

1.3. Paper organization

This paper is structured as follows. Section 2 provides the model description. Section 3 presents the solution strategy for obtaining numerical results. Section 4 details the data we used as well as our assumptions. Section 5 reviews our analysis metrics. Section 6 discusses results while Section 7 concludes.

2. Model description

The model presented in this section is a simultaneous-move, one-shot, noncooperative game in which agents are coupled through market clearing as well as other constraints that ensure network integrity. Firstly, we provide an overview of the modelling approach in Section 2.1. Secondly, we detail the mathematical formulation of the decision problem of each agent in Section 2.2.

2.1. Modelling approach

We emulate a long-run equilibrium, between consumers and producers, on a perfectly competitive electricity market, assuming complete integration of wholesale and retail. In all market designs, concurrent to the electricity market, we also consider an ancillary service market for regulation of reactive power. Market participants have perfect information and are price takers. We use a Nash game framework, analysing the strategic interactions between self-interested consumers and large-scale producers. Through this modelling approach, we thus find the long-run Nash equilibrium where production is attained at lowest possible cost and system social welfare is maximized. A diagram providing a general overview of the market structure considered in the model can be found in Fig. 2.

The considered market participants are large scale generators and residential consumers. Generators are not located in the LVDS, we place them at the slack node which represents higher voltage levels (*i.e.* transmission level), on the other hand, residential consumers are located on nodes throughout the LVDS. The large scale generators comprise three conventional assets, generalized as a base-load, mid-load and peak-load technologies, as well as a renewable generator, namely, a wind farm. Residential consumers are categorized as small (single household in a detached house) or large (multiple households in a condominium). We highlight that the latter is one entity, having a load that is the sum of that of all households in the building. All consumers have the ability to invest in a BESS as well as a solar PV

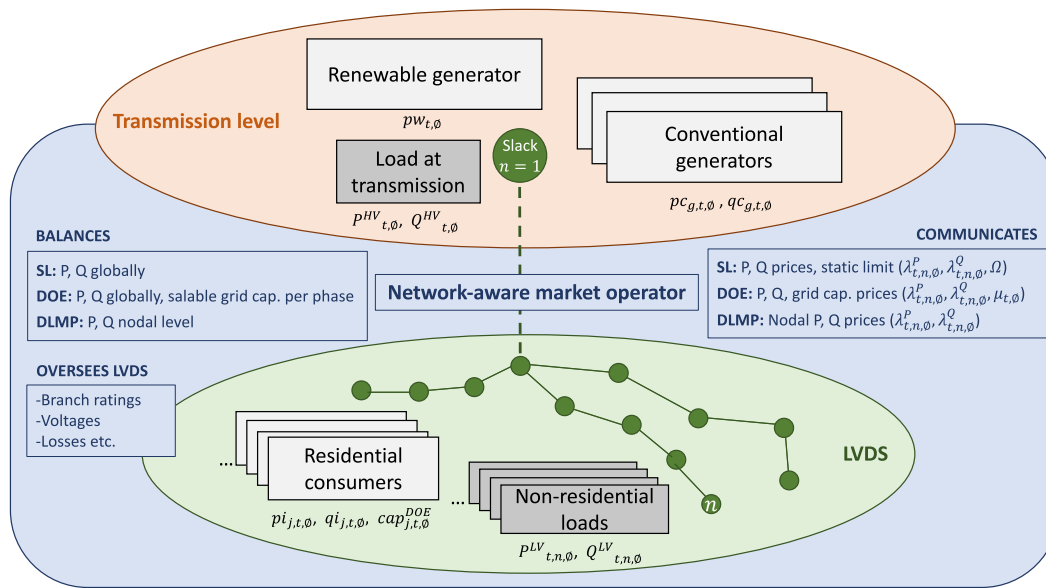


Fig. 2. Overview of market structure. Market agents in light grey boxes, exogenous inputs in dark grey boxes. Variables/parameters that each agent can communicate to the network-aware market operator are illustrated. The network-aware market operator balances markets, safeguards LVDS network constraints and communicates prices and/or limit depending on market design.

system, the size of the assets they can invest in is proportional to the number of households they represent.

To endogenise the wholesale price we also include a transmission level load, at the slack node, reflecting demand occurring at higher voltage levels. Throughout the LVDS there also exist small commercial loads and loads from street-lighting, garages, lifts and the like. These are all parameters within our model.

All agents are given annualized investment cost values. Thus, their operational and investment decisions are made for an entire year, assuming that these costs will remain the same for the lifetime of the asset they invest in. Agents are interlinked via a series of constraints that ensure that supply meets demand and that LVDS network limits (such as branch ratings and voltage bounds) are respected. These constraints fall within the competences of, what we term, a ‘network-aware market operator’. The market operator determines active and reactive power prices on an hourly basis with no price caps being imposed. Consumers and generators pay or are remunerated according to these hourly prices for imports and exports. In the DLMP-based market design these prices are nodal and convey information on local network status, guiding consumers to respect network limits. To ensure network integrity in SL-based design, the network-aware market operator communicates a static limit, equivalent across all phases, to all residential consumers, and in the DOE-based design communicates an hourly, per-phase grid capacity price, determined from an aggregate amount of capacity that, regardless of how it is distributed, ensures a network-admissible solution.

While we do not account for the physical constraints of the transmission network, considering dispatch and investment decisions related to large-scale generation technologies located at the transmission level captures their influence on wholesale price formation. Importantly, our modelling approach allows for the interaction between distribution and transmission level decisions, both operational and investment, providing a comprehensive perspective on price formation at the distribution level. This differs from analyses in which wholesale electricity prices are static and unaffected by distribution level decisions.

2.2. Mathematical formulation

In this section, the decision-making problem of each agent is presented in detail. Except for the market operator, all agents’ decision

problems are cast as optimization problems. The market operator imposes design-specific linking constraints that maintain (1) market balance and (2) network integrity. These constraints must be satisfied by the solutions of other agents’ individual optimization problems. Thus, the market operator links the decisions of all agents, ensuring overall market clearing and network management.

Where relevant, dual variables associated with a constraint are given between brackets. Uppercase letters are used to denote parameters (exogenous to the model) while lowercase letters to denote variables (endogenous to the model). Each consumer has either a single-phase or three-phase connection to the grid. A consumer’s phases are thus denoted by the set $\Phi_j \subseteq \Phi$. For clarity’s sake we omit consumer j and generator g indices in the mathematical description of the decision problem of the respective agents. Acronyms **SL**, **DOE**, **DLMP** and **A**, found in front of equations, denote whether the equation in question is part of SL-based design, DOE-based design, DLMP-based design or is common to all three.

2.2.1. Consumer problem

Residential consumers, as price-takers with inelastic demand, aim to minimize costs, which vary based on market design. In SL and DLMP-based designs, the consumer’s objective function is shown in (1), while (2) illustrates the function under DOE-based design. Both objectives feature terms representing the consumer’s interaction with energy and ancillary service markets. Active power can be imported or exported via variable $p_{i,t,\phi}$ and reactive power via $q_{i,t,\phi}$. Imports and exports are valued at prices $\lambda_{i,n,\phi}^P$ and $\lambda_{i,n,\phi}^Q$, respectively. It is important to note that, in the DLMP-based design, prices may differ across the network’s nodes and phases, this is not the case in SL and DOE-based designs in which we leave the indices n and ϕ , yet no spatial differentiation of prices occurs. Additionally, (2) includes a term representing the cost of network capacity. Consumers can purchase per-phase network capacity, $cap_{i,\phi}^{DOE}$, hourly at price $\mu_{t,\phi}$, affecting their import/export capability. All residential consumers have the option to invest in both a BESS and a solar PV system, with separate inverters for independent sizing decisions. They choose the total solar PV panel capacity and solar inverter capacity, as well as the battery capacity and inverter capacity for the BESS, according to the perceived, annualized investment cost of each.

Eqs. (4) to (8) outline the operation of the consumer's solar PV system. The total installed solar PV panel capacity must not exceed the available roof space (4). Active power generation is limited by the product of installed panel capacity and solar availability factor (5), accounting for orientation. Each consumer has an assumed roof orientation (south, east or west). Active power output is further constrained by the installed solar inverter capacity (6). Inequality constraints, (5) and (6), enable the consumer to curtail solar PV output and adhere to export/import limits. Reactive power generation or absorption is managed by the smart inverter (7). This equation is linearized as done by Attarha et al. [21], using 24 linear segments to overestimate the circle with at most 0.001% error. Reactive power adjustments are only allowed during active power generation (8).

Eqs. (9) to (18) define the consumer's BESS, establishing investment limits (9)–(10), energy content constraints (11)–(12), operational limits (13)–(14), and net power exchange (15). Eqs. (16) to (18) enforce cyclical boundary conditions, ensuring that the BESS's energy content corresponds to a specific state of charge, $SOCE$, at the end of each day. Consumers manage their BESS with the objective to minimize their overall cost, while ensuring compliance with inter-temporal and capacity constraints.

Eqs. (19) and (20) govern the behind-the-meter active and reactive power balances of the consumer. Power exchange with the grid is determined by the difference between the consumer's load³ and the power generated or absorbed by their BESS and solar PV system. For three-phase consumers, export/import operations occur on each phase, assuming that such consumers have three-phase inverters with power distribution balanced across phases [38]. This approach is enforced mathematically by dividing the respective terms by the number of phases $|\Phi_j|$ and aligns with existing standards [39], in which prosumers are obliged to minimize their phase imbalance from DER.

The remaining constraints are market design specific. Eqs. (21) and (24) are part of the SL-based design, where consumer exports and imports are bound by an equivalent limit denoted as Ω . This limit, in kW, set by the market operator, ensures network limits are respected. We assume that import and export limits are symmetrical. Only in the rare event of the limit falling short of their inelastic demand, consumers retain the ability to import up to their demand. Eqs. (25) to (29) belong to the DOE-based design, where consumers purchase per-phase network capacity, $cap_{t,\phi}^{DOE}$, to use for import or export. Under this design, consumers can adjust their export/import levels hourly. Their imports are limited by the purchased capacity plus their demand, this ensures that consumers can always fulfil their inelastic demand, even in cases of network capacity scarcity or monopolization on behalf of other consumers. In all constraints pertaining to reactive power, we use a power factor of 0.95, denoted as κ , indicating that a portion of either SL or DOE can be allocated to importing/exporting reactive power, similar to the approach in [16]. Finally, in the DLMP-based design, locational price signals ensure operations remain within network limits, with no additional constraints on consumer grid interactions.⁴

$$\boxed{\text{SL}} \boxed{\text{DLMP}} \min \sum_{t \in \mathcal{T}} \sum_{\phi \in \Phi_j} \left(\lambda_{t,n,\phi}^P \cdot p_{t,\phi} + \lambda_{t,n,\phi}^Q \cdot q_{t,\phi} \right) + \text{investments} \quad (1)$$

$$\boxed{\text{DOE}} \min \sum_{t \in \mathcal{T}} \sum_{\phi \in \Phi_j} \left(\lambda_{t,n,\phi}^P \cdot p_{t,\phi} + \lambda_{t,n,\phi}^Q \cdot q_{t,\phi} + \mu_{t,\phi} \cdot cap_{t,\phi}^{DOE} \right) + \text{investments} \quad (2)$$

³ For large consumers, the aggregate of all households' loads in the building.

⁴ In reality there exists a physical limit: the consumers' connection capacity or fuse rating. We assume that this fuse rating is non-binding.

$$\text{investments} = IC^{PV} \cdot cap^{PV} + IC^{PV_i} \cdot cap^{PV_i} + IC^S \cdot cap^S + IC^{Si} \cdot cap^{Si} \quad (3)$$

$$\boxed{\text{A}} \quad 0 \leq cap^{PV} \leq CAP^{PV} \quad (4)$$

$$\boxed{\text{A}} \quad 0 \leq ppv_t \leq cap^{PV} \cdot AF_{t,o}^{PV} \quad \forall t \in \mathcal{T} \quad (5)$$

$$\boxed{\text{A}} \quad 0 \leq cap^{PV_i} \leq cap^{PV} \quad (6)$$

$$\boxed{\text{A}} \quad ppv_t^2 + qpvt^2 \leq (cap^{PV_i})^2 \quad \forall t \in \mathcal{T} \quad (7)$$

$$\boxed{\text{A}} \quad -ppv_t \leq qpvt \leq ppv_t \quad \forall t \in \mathcal{T} \quad (8)$$

$$\boxed{\text{A}} \quad 0 \leq cap^S \leq CAP^S \quad (9)$$

$$\boxed{\text{A}} \quad 0 \leq cap^{Si} \leq cap^S \quad (10)$$

$$\boxed{\text{A}} \quad e_t \geq cap^S \cdot \underline{SOC} \quad \forall t \in \mathcal{T} \quad (11)$$

$$\boxed{\text{A}} \quad e_t \leq cap^S \cdot \overline{SOC} \quad \forall t \in \mathcal{T} \quad (12)$$

$$\boxed{\text{A}} \quad 0 \leq ch_t \leq cap^{Si} \quad \forall t \in \mathcal{T} \quad (13)$$

$$\boxed{\text{A}} \quad 0 \leq dc_t \leq cap^{Si} \quad \forall t \in \mathcal{T} \quad (14)$$

$$\boxed{\text{A}} \quad ps_t = ch_t - dc_t \quad \forall t \in \mathcal{T} \quad (15)$$

$$\boxed{\text{A}} \quad e_t = cap^S \cdot SOC^E \quad t = T \quad (16)$$

$$\boxed{\text{A}} \quad e_t = cap^S \cdot SOC^E + \left(ch_t \cdot \eta^{ch} - \frac{dc_t}{\eta^{dc}} \right) \quad t = 1 \quad (17)$$

$$\boxed{\text{A}} \quad e_t = e_{t-1} + \left(ch_t \cdot \eta^{ch} - \frac{dc_t}{\eta^{dc}} \right) \quad \forall t \in \mathcal{T} \setminus 1 \quad (18)$$

$$\boxed{\text{A}} \quad pi_{t,\phi} = P_{t,\phi} - \frac{ppv_t}{|\Phi_j|} + \frac{ps_t}{|\Phi_j|} \quad \forall t \in \mathcal{T}, \phi \in \Phi_j \quad (19)$$

$$\boxed{\text{A}} \quad qi_{t,\phi} = Q_{t,\phi} - \frac{qpvt}{|\Phi_j|} \quad \forall t \in \mathcal{T}, \phi \in \Phi_j \quad (20)$$

$$\boxed{\text{SL}} \quad pi_{t,\phi} \geq -\Omega \quad \forall t \in \mathcal{T}, \phi \in \Phi_j \quad (21)$$

$$\boxed{\text{SL}} \quad qi_{t,\phi} \geq -\Omega \cdot F \quad \forall t \in \mathcal{T}, \phi \in \Phi_j \quad (22)$$

$$\boxed{\text{SL}} \quad pi_{t,\phi} \leq \begin{cases} \Omega & \text{if } \Omega \geq P_{t,\phi} \\ P_{t,\phi} & \text{otherwise} \end{cases} \quad \forall t \in \mathcal{T}, \phi \in \Phi_j \quad (23)$$

$$\boxed{\text{SL}} \quad qi_{t,\phi} \leq \begin{cases} \Omega \cdot F & \text{if } \Omega \cdot F \geq Q_{t,\phi} \\ Q_{t,\phi} & \text{otherwise} \end{cases} \quad \forall t \in \mathcal{T}, \phi \in \Phi_j \quad (24)$$

$$\boxed{\text{DOE}} \quad 0 \leq cap_{t,\phi}^{DOE} \quad \forall t \in \mathcal{T} \quad (25)$$

$$\boxed{\text{DOE}} \quad pi_{t,\phi} \leq cap_{t,\phi}^{DOE} + P_{t,\phi} \quad \forall t \in \mathcal{T}, \phi \in \Phi_j \quad (26)$$

$$\boxed{\text{DOE}} \quad qi_{t,\phi} \leq (cap_{t,\phi}^{DOE} \cdot F) + Q_{t,\phi} \quad \forall t \in \mathcal{T}, \phi \in \Phi_j \quad (27)$$

$$\boxed{\text{DOE}} \quad pi_{t,\phi} \geq -cap_{t,\phi}^{DOE} \quad \forall t \in \mathcal{T}, \phi \in \Phi_j \quad (28)$$

$$\boxed{\text{DOE}} \quad qi_{t,\phi} \geq -cap_{t,\phi}^{DOE} \cdot F \quad \forall t \in \mathcal{T}, \phi \in \Phi_j \quad (29)$$

$$\text{where } F = \frac{\sqrt{1 - \kappa^2}}{\kappa} \quad (30)$$

2.2.2. Conventional generator problem

We assume conventional generators are three-phase connected at transmission/higher voltage levels (represented by the slack node, $n = 1$). They aim to maximize profits as outlined in (31). Profit is derived from selling active, $pc_{t,\phi}$, and reactive power, $qc_{t,\phi}$, at market prices, subtracting operational and investment costs. Operational costs, proportional to variable generation costs (VC^P , VC^Q), and investment costs, based on capacity investment, cap^C , and annualized investment cost, IC^C , are considered. Generator capacity, cap^C , determines active power generation limits (33). We assume that these large synchronous

generators are required to generate reactive power and do so maintaining a minimum power factor, κ , of 0.90, as enforced by (35), as in [32].

$$\boxed{\text{A}} \max \sum_{t \in \mathcal{T}} \sum_{\phi \in \Phi} \left((\lambda_{t,n,\phi}^P - VC^P) p c_{t,\phi} + (\lambda_{t,n,\phi}^Q - VC^Q) q c_{t,\phi} \right) - IC^C \cdot cap^C \quad (31)$$

$$\boxed{\text{A}} 0 \leq cap^C \quad (32)$$

$$\boxed{\text{A}} 0 \leq p c_{t,\phi} \leq cap^C \quad \forall t \in \mathcal{T}, \phi \in \Phi \quad (33)$$

$$\boxed{\text{A}} 0 \leq q c_{t,\phi} \quad \forall t \in \mathcal{T}, \phi \in \Phi \quad (34)$$

$$\boxed{\text{A}} q c_{t,\phi} \leq \frac{p c_{t,\phi} \cdot \sqrt{1 - \kappa^2}}{\kappa} \quad \forall t \in \mathcal{T}, \phi \in \Phi \quad (35)$$

2.2.3. Renewable generator problem

Like conventional generators, we assume the renewable generator is three-phase connected at higher voltage levels (represented by the slack node, $n = 1$). The renewable generator's objective consists in maximizing profit (36). Profit is the revenues made from selling active power, $p w_{t,\phi}$, at the prevailing market price, minus the investment cost, equal to the amount of capacity that is invested in, cap^W , times the annualized capacity investment cost IC^W . We assume that the renewable generator has no variable costs. The invested capacity, and weather conditions, embodied by the availability factor, AF_t^W , limit the active power output of the generator (38).

$$\boxed{\text{A}} \max \sum_{t \in \mathcal{T}} \sum_{\phi \in \Phi} \left(\lambda_{t,n,\phi}^P \cdot p w_{t,\phi} \right) - IC^W \cdot cap^W \quad (36)$$

$$\boxed{\text{A}} 0 \leq cap^W \quad (37)$$

$$\boxed{\text{A}} 0 \leq p w_{t,\phi} \leq cap^W \cdot AF_t^W \quad \forall t \in \mathcal{T}, \phi \in \Phi \quad (38)$$

2.2.4. Market operator constraints

We consider a network-aware market operator responsible for balancing energy and ancillary service markets while safeguarding the physical limitations of the grid. The manner in which the market operator will attain demand–supply equilibrium and achieve network admissible operation is dependent upon the market design.

SL-based design. The market operator ensures a global balance of active and reactive power according to (39) and (40). These equations dictate that the aggregate generation from large-scale generators and non-residential demand at various voltage levels matches the sum of net consumer off-take per phase, per time-step. The wholesale prices $\lambda_{t,n,\phi}^P$ and $\lambda_{t,n,\phi}^Q$ that determine the balance are the dual variables of (39) and (40). These prices remain spatially uniform across nodes and phases. To safeguard voltage and thermal limits, the market operator sets the magnitude of Ω in the consumer's problem (21).

$$\boxed{\text{SL}}, \boxed{\text{DOE}} \sum_{j \in \mathcal{J}} p i_{j,t,\phi} = \sum_{g \in \mathcal{G}} (p c_{g,t,\phi}) + p w_{t,\phi} + P_{t,\phi}^{HV} + \sum_{n \in \mathcal{N}} P_{t,n,\phi}^{LV} (\lambda_{t,n,\phi}^P) \quad \forall t \in \mathcal{T}, \phi \in \Phi \quad (39)$$

$$\boxed{\text{SL}}, \boxed{\text{DOE}} \sum_{j \in \mathcal{J}} q i_{j,t,\phi} = \sum_{g \in \mathcal{G}} (q c_{g,t,\phi}) + Q_{t,\phi}^{HV} + \sum_{n \in \mathcal{N}} Q_{t,n,\phi}^{LV} (\lambda_{t,n,\phi}^Q) \quad \forall t \in \mathcal{T}, \phi \in \Phi \quad (40)$$

DOE-based design. The market operator ensures global power balance, as done in SL-based design, by (39) and (40). Additionally, an hourly market for grid capacity is established, with the operator determining the aggregate purchasable amount and the grid capacity price $\mu_{t,\phi}$. The tradable network capacity, governed by (41), maintains network integrity, with the sum of purchased capacity by consumers constrained by Ω , representing a certain amount of individual capacity in kW, multiplied by the number of residential consumers connected to the network in that phase, N^ϕ . The price $\mu_{t,\phi}$, the dual of (41), is non-zero when the constraint is binding. Consumers' acquisition of grid capacity is dependent upon their willingness to pay for $cap_{t,\phi}^{DOE}$.

$$\boxed{\text{DOE}} \sum_{j \in \mathcal{J}} cap_{j,t,\phi}^{DOE} \leq N^\phi \cdot \Omega (\mu_{t,\phi}) \quad \forall t \in \mathcal{T}, \phi \in \Phi \quad (41)$$

DLMP-based design. The market operator communicates DLMPs to all agents. These reflect the marginal cost of energy, congestion, losses and voltage issues at each node and phase of the network. To derive DLMPs the market operator enforces power flow constraints. The dual of the nodal balance constraints for active and reactive power formally give $\lambda_{t,n,\phi}^P$ and $\lambda_{t,n,\phi}^Q$. In this paper we utilize the forward–backward sweep (FBS) linearization of the nonlinear, non-convex AC power flow constraints, formulated by [40], available in the Julia package *PowerModelsDistribution.jl* as *FBSUBFPowerModel* [41]. To this formulation we add branch power rating constraints which we linearize by means of an inner approximation of a circle, explained in further detail in Appendix A.

3. Solution strategy

To solve the equilibrium problem between producers and consumers in each market design, the mixed complementarity problem (MCP) formed from the optimization problems of each agent linked together via coupling constraints enforced by the network-aware market operator, is recast into a single optimization problem as outlined in [42]. This so called equivalent optimization problem (EOP), comprises all constraints from the individual optimization problems of each agent and aims to minimize the aggregate costs present in the system. By solving this optimization problem, we identify a Nash equilibrium. In this equilibrium state, no single agent can unilaterally improve their outcome given the strategies of the other agents, reflecting the optimal allocation of resources and maximization of system social welfare. Each market design has its own EOP, namely EOP_{SL} , EOP_{DOE} and EOP_{DLMP} . It is interesting to note that EOP_{DLMP} corresponds to an optimal power flow (OPF) problem. The specific OPF is a quadratic program. While all constraints are linear there exist quadratic terms in the objective, which will be expounded upon in detail in the subsequent section. On the other hand, EOP_{SL} and EOP_{DOE} are both linear programs. Utilization of quadratic and linear programs is a deliberate choice so duals may be readily interpretable as prices. For the full description of each EOP the reader is directed to Appendix B. In the following sections we detail the process of achieving AC feasible solutions within each market design (Section 3.1) and discuss the integration of network losses for both SL and DOE-based designs in Section 3.2.

3.1. AC feasibility

To ensure network-admissible solutions under an AC power flow formulation, various methods are employed. For simpler designs, the focus is on determining the largest feasible value of Ω , while for DLMP-based design, an iterative approach is utilized with the linear power flow formulation to achieve an AC feasible solution.

3.1.1. Parametrization of Ω

In SL and DOE-based designs, to provide network admissible limits or grid capacity, the network-aware market operator sets Ω . In practice, we find the full range of Ω yielding AC feasible market equilibria, using the following iterative approach:

- (1) *Initialization*: Set $\Omega = 0$ kW
- (2) *Solve EOP*: Solve the design's EOP, to find the market equilibrium under the set Ω , yielding optimal investment and operational decisions of all agents.
- (3) *Check AC feasibility*: With the hourly active and reactive power generation and consumption decisions of agents run an AC power flow simulation using the *PowerModelsDistribution.jl* package [41]. Check for voltage and branch rating violations. If violations are found, then stop, the previous Ω , was the maximum value guaranteeing safe grid operation.
- (4) *Update Ω* : If no violation occurred, increase Ω by 0.01 kW and repeat steps (2) and (3).

3.1.2. Successive approximation

In the DLMP-based design, the FBS linearization of power flow constraints can either directly replace AC power flow constraints for an approximate solution or be used as part of an iterative, successive approximation approach to yield an AC feasible solution upon convergence [40]. We employ the latter approach. The successive approximation is carried out using the following steps:

- (1) *Initialization*: Set iteration count $k = 0$ and use a flat-start, whereby $V^{k=0} = |\mathbf{V}| \angle \boldsymbol{\theta} = [1 \angle 0^\circ \quad 1 \angle -120^\circ \quad 1 \angle 120^\circ]^T$, as an initial voltage estimate for all voltages.
- (2) *Solve EOP*: Solve EOP_{DLMP} , in which the voltage estimate is used to linearize the appropriate power flow equations. The solution yields a new voltage estimate V^{k+1} .
- (3) *Check convergence*: Check if the stopping criterion, ϵ , which defines a suitable deviation between V^k and V^{k+1} , is satisfied. If so, stop, the solution is AC feasible.
- (4) *Update voltage estimate*: If the stopping criterion is not satisfied, update the voltage estimate and repeat steps (2) and (3). The voltage estimate is updated using $V^k = V^{k+1}$.

To promote convergence, quadratic terms are incorporated into the objective function of EOP_{DLMP} , penalizing deviations in both active and reactive power export/import of consumers from the previous iteration. This approach draws inspiration from the work of [40]. Eqs. (42) and (43) define these penalty terms, in which the superscript k denotes the iteration and the term ρ^k is a small weighting factor.

$$P_{pen} = \sum_{i \in \mathcal{T}} \sum_{j \in \mathcal{J}} \sum_{\phi \in \Phi} \left(p_{j,i,\phi}^k - p_{j,i,\phi}^{k-1} \right)^2 \cdot \rho^k \quad (42)$$

$$Q_{pen} = \sum_{i \in \mathcal{T}} \sum_{j \in \mathcal{J}} \sum_{\phi \in \Phi} \left(q_{j,i,\phi}^k - q_{j,i,\phi}^{k-1} \right)^2 \cdot \rho^k \quad (43)$$

3.2. Accounting for network losses

In the DLMP-based design, the presence of losses is accounted for within the optimization problem by the embedded power flow constraints, this is not the case for SL or DOE-based design. As such, we estimate a cost of losses using the results of the ex-post AC power flow simulation performed to check the AC feasibility of these designs. This estimated cost of losses is added to the resulting objective of the respective EOP to derive a total system cost that allows for a fair comparison between all market designs.

The estimated cost of losses, C^{loss} , has two components: C^{gen} , the cost of additional generation needed to balance losses and C^{cap} , the cost of generation capacity investments needed to provide the additional generation, as exemplified in (44). We value additional generation at the appropriate market price (45). The terms P_i^{loss} and

Q_i^{loss} represent the sum of active and reactive series losses occurring in the network at a specific time-step. In DOE and SL-based design, prices are uniform across nodes and phases, as such the indices n and ϕ in prices may be disregarded. Furthermore, we value supplementary generation capacity, CAP^{extra} , at the annualized investment cost of our peak-load generation technology (46). To evaluate if supplementary generation capacity is needed we check that the sum of generation plus losses, at every time step does not exceed available generation capacity.

$$C^{loss} = C^{gen} + C^{cap} \quad (44)$$

$$C^{gen} = \sum_{i \in \mathcal{T}} \lambda_{i,n,\phi}^P \cdot P_i^{loss} + \lambda_{i,n,\phi}^Q \cdot Q_i^{loss} \quad (45)$$

$$C^{cap} = IC^{peak} \cdot CAP^{extra} \quad (46)$$

4. Case study: data and assumptions

The performed case study is largely based on Belgian input data, using 2030 cost assumptions. We model an entire year with hourly temporal resolution. For computational tractability however, we make use of 12 representative days. Representative days were selected using the optimization problem outlined in [43], leveraging the Julia package *RepresentativePeriodsFinder.jl* [44]. As inputs to the optimization problem we provide some of the time series data that is henceforth described.

4.1. Time series data

The time series data employed in this study comprises availability factors for solar PV and wind energy resources, along with demand data. Availability factors are sourced from [45], in which current as well as potential generation for Belgian residential solar PV and wind installations is mapped. Specifically, availability factors are provided for south, east, and west-facing solar panels, with each residential consumer being randomly assigned one. Additionally, in each network, each residential consumer is allocated a demand profile from a set of 1200 profiles generated using the open-source web tool developed by Baetens and Saelens [46]. This tool models residential occupant behaviour based on Belgian statistical data, encompassing active power demand for lighting, large and small appliances, and electronics.

To incorporate demand occurring at higher voltage levels, we scale Elia's active power grid load data from 2017 to match the weather year utilized in load profile generation [47]. The scaling is adjusted to be proportional to the number of households in the network in question, accounting for Belgium's approximate 5 million households. Additionally, within the LVDS, non-residential loads such as small commercial, street lighting, and schools are present. Given the scarcity of available demand data on these loads, we adopt the assumption that their demand remains constant and equal to their grid connection capacity. Across all loads, we presume a power factor of 0.95 to calculate reactive power demand and we evenly distribute demand across the phases of the load's connection point. Within the LVDS, both residential and non-residential consumers are connected in either single-phase or three-phase. The higher voltage load is spread across three phases and placed at the network's slack node. For the generation of representative days, availability factors and higher voltage demand data were utilized.

4.2. DER parameters

All solar PV capacity is exclusively installed at residential level, in the form of grid-connected, roof-mounted systems. The capacity limit, CAP_j^{PV} , for solar PV installations stands at 10 kW for small consumers. For large consumers, it scales proportionally with the number of households they encompass. The largest condominium in the LVDS being allocated a CAP_j^{PV} of 100 kW. These installation sizes align with those observed in Belgium [48]. We project 2030 solar PV system costs

Table 1

Techno-economic parameters for residential solar PV and BESS. The data source is shown as either a reference or own model assumption (MA). Listed investment costs are not annualized.

Parameter	Symbol	Unit	Value	Source
Solar PV				
Investment cost		€/kW	481	[52]
Lifetime		years	25	[53]
PV Inverter				
Investment cost		€/kW	96	[52]
Lifetime		years	15	[53]
BESS				
Investment cost		€/kWh	153	[49]
Lifetime		years	18	[49]
Charging efficiency	η^{ch}	%	95	[49]
Discharging efficiency	η^{dc}	%	95	[49]
Min state of charge	$\frac{SOC}{SOC}$	%	20	MA
Max state of charge	$\frac{SOC}{SOC}$	%	90	MA
State of charge day's end	SOC^E	%	50	MA
BESS Inverter				
Investment cost		€/kW	56	[49]
Lifetime		years	20	[49]
Common				
Discount rate		%	3–7	[50]

based on 2019 data using the learning curve (LC) method detailed in Appendix C.

Similarly, all storage capacity is installed at residential level. We establish installation capacity limits, CAP_j^S , of 13.5 kWh for small consumers, resembling a typical Tesla PowerWall. While for large consumers, the capacity limit scales with the number of households, with the largest condominium granted a CAP_j^S of 200 kWh. Considering an Energy-to-power (E/P) ratio of 1, these sizes are in line with those found in [49] for residential storage.

All costs are annualized⁵ to derive model inputs, IC_j^{PV} , IC_j^{PVi} , IC_j^S and IC_j^{Si} , representing consumers' perceived, annualized investment costs in 2030. We consider varying investment risks and opportunity costs, assigning a random discount rate between 3% and 7% to each consumer [50]. All techno-economic parameters for solar PV and BESS are detailed in Table 1 with their appropriate sources.⁶

4.3. Large scale generator parameters

All other generation capacity is installed at higher voltage levels, represented by the slack node of each LVDS ($n = 1$). For these generators we take data from [54], considering one renewable technology, namely a wind farm, and three conventional technologies generalized as base, mid and peak-load generators. These broad technology classes are used such that no fundamentally different insights would be gained by increasing the complexity of the model with more technologies. In Table 2 the variable as well as annualized investment costs are shown. Shown in Table 2 is the variable cost for active power generation, we assume that of reactive power to be 1% of this. A common rule of thumb in literature is that the reactive power price is below 1% of the active power price [55].

4.4. Network data

The 14 networks utilized in this study are a subset of a comprehensive, real (non-synthetic) LVDS representative of a typical European town's network, sourced from [56]. Each of these networks represents a distinct segment, below individual substations, within the larger LVDS. Overall, the LVDS is a TT grounded, three-phase, four-wire grid, that,

Table 2

Variable (VC^P) and annualized investment (IC^C) costs of the considered large scale generation technologies.

Source: Taken from [54].

Technology	Variable [€/MWh]	Investment [€/MW]
Base	36	138,000
Mid	53	82,000
Peak	76	59,000
Wind	0	76,500

for modelling purposes was reduced to an equivalent three-wire system. All substations are connected to a single, nearly infinite source (slack node) and all loads have either three-phase or single-phase connection. Further detail on these networks can be found in Appendix D.

For each network under investigation, we run each market design 10 times, assigning always different discount rates and demand profiles from the set of 1200 profiles that were created. We term these different 'consumer placements'. As such, we analyse a total of 140 cases per market design. Lower and upper voltage bounds are set to 0.90 and 1.05 per unit.⁷ In DLMP-based design, we define the stopping criterion ϵ , the deviation in voltage between iterations, to be 1×10^{-4} . For a detailed discussion on the computational complexity involved in finding the equilibrium in each market design across different networks and consumer placements, please refer to Appendix E.

4.5. DSO cost recovery

Recognizing that in DLMP-based design the price signal encompasses components beyond the energy price, payable to the DSO and that in DOE-based design the same occurs with payments of network capacity, we make the assumption that, irrespective of market design, the DSO needs to recover, in total, an amount of 400 € per consumer annually, as done in [57]. While this specific cost is not explicitly integrated into our model, it is employed in ex-post calculations to allow for a comparative assessment of the costs faced by consumers in each design.

These 400 €/yr per consumer, can be recuperated through a combination of variable and fixed payments, contingent upon the market design. Under a DOE-based design, consumers make payments to the DSO for grid capacity. In a DLMP-based design, consumers compensate the DSO/are remunerated by the DSO based on the network price component of the DLMP and their interaction with the grid. Both of these entail variable payments made by individual consumers, contributing to the DSO's cost recovery and mitigating the need for a fixed component. Thus, in these designs, consumers make variable payments in addition to a fixed payment used to make sure the DSO recovers, in total, 400 €/yr per consumer. In contrast, under the SL-based design, each consumer simply pays a fixed annual fee of 400 €.

5. Metrics

We now introduce a series of metrics utilized in our results analysis. In Section 5.1 we introduce the metric of Consumer Type Distribution Index (CTDI), used within results to classify networks. In Section 5.2 we describe the concept of Per Consumer Capacity (PCC), a metric for standardizing the measurement of given grid capacity across DOE and SL-based designs. In Section 5.3 we clarify what total system cost represents.

⁷ We set tighter upper voltage bounds, to prioritize avoiding overvoltage scenarios, which are typically more critical in terms of system stability and equipment protection, especially given the hourly resolution of our model.

⁵ Annual cost = $\frac{\text{Asset cost} \times \text{Discount rate}}{1 - (1 - \text{Discount rate})^{\text{lifetime}}}$

⁶ BESS-related costs are converted from source using the average 2017 exchange rate of 1 EUR = 1.13 USD [51].

5.1. Consumer type distribution index

We introduce a metric, named the consumer type distribution index (CTDI), to assess the spatial distribution of consumer types along electrical feeders in each network and therefore categorize the spectrum of networks under analysis. The CTDI is defined as the weighted average of the ratio of the number of small consumers, N_{small} , to the total number of consumers, $N_{small} + N_{large}$, for each feeder in the network, where the weights are the lengths of the feeders. The formula for the CTDI of a network is given by (47)–(48) where F denotes the set of feeders in the network.

$$CTDI = \frac{\sum_{f \in F} \text{Feeder length} \times \text{Consumer factor}}{\sum_{f \in F} \text{Feeder length}} \quad (47)$$

$$\text{Consumer Factor} = \frac{N_{small}}{N_{small} + N_{large}} \quad (48)$$

A higher CTDI value indicates that the network is characterized by longer feeders, and these longer feeders have a larger proportion of small consumers relative to large consumers. On the other hand, a lower CTDI suggests that the network consists of shorter feeders, and these shorter feeders have a higher proportion of large consumers or condominiums.

5.2. Per consumer capacity

In both DOE-based design and SL-based design, the parameter Ω defines, in the modelling approach, the per consumer amount of useable grid capacity.⁸ In SL-based design, Ω is translated to consumer export and import limits. In DOE-based design, it is translated to an aggregate, network-level capacity available for purchase by consumers such that they may export power to the grid or supplement their withdraw capability. Although the meaning of Ω remains consistent, its range differs between these two designs. As such, we introduce the term per consumer capacity (PCC) to specify Ω , normalized within each design to the range of 0 to 1. This normalization allows for a standardized comparison, facilitating assessment on the implications that the relative amount of useable capacity has on results.

5.3. Total system cost

In this study, total system cost (TSC) is used as an indicator of economic efficiency for each market design. Total system cost is composed of: (1) capital expenditure (CAPEX) in DER, meaning all consumer investments in solar PV, BESS and respective inverters (2) CAPEX in large-scale generators (3) operational expenditure (OPEX) of large-scale generators, meaning the variable cost of running the conventional generation technologies:

$$\begin{aligned} TSC = & \text{CAPEX DER} + \text{CAPEX large-scale generators} \\ & + \text{OPEX large-scale generators} \end{aligned} \quad (49)$$

$$\begin{aligned} TSC = & \sum_{j \in J} \left(IC_j^{PV} \cdot cap_j^{PV} + IC_j^{PVi} \cdot cap_j^{PVi} \right. \\ & \left. + IC_j^S \cdot cap_j^S + IC_j^{Si} \cdot cap_j^{Si} \right) \\ & + \sum_{g \in G} \left(IC_g^C \cdot cap_g^C \right) + IC^W \cdot cap^W \\ & + \sum_{g \in G} \sum_{i \in I} \sum_{\phi \in \Phi} \left(VC_g^P \cdot pc_{g,t,\phi} + VC_g^Q \cdot qc_{g,t,\phi} \right) \end{aligned} \quad (50)$$

⁸ Not be confused with the physical capacity of network branches.

6. Results

The following sections detail the case study's results. Considering a single case, we first clarify what signals consumers perceive in each market design and how this affects their investment as well as operational decisions (Section 6.1). Subsequently, in Section 6.2, the analysis considers all cases (networks and consumer placements), in order to assess how the three market designs drive variations in system-level outcomes.

6.1. Consumer perspective

Across the investigated market designs, consumers are exposed to various signals, prompting different investment and operational decisions. The DLMP encourages large solar PV installations and significant energy injections. The network capacity price in DOE-based design results in substantial variations in who injects energy and owns DER. In contrast, the static limit homogenizes consumer decisions.

In DLMP-based design, consumers are exposed to a composite price known as DLMP, which includes both the energy price and other components reflecting network constraints. We collectively term these as a 'network price'. The energy price, set in our model at the slack node ($n = 1$), remains uniform across the network (although it may vary across phases), whereas the network price is location-specific and can vary by node and phase. Negative network prices indicate that within the LVDS, network infrastructure is nearing its capacity due to excess generation or insufficient demand.⁹ Conversely, positive network prices suggest insufficient generation or high demand.¹⁰ Operationally, negative network prices prompt consumers to increase consumption or reduce injection, while positive prices prompt the opposite behaviour. Fig. 3 illustrates five consumers, of type small, that are distributed across a network. The figure details: their DER investments, their active power injection (green) or withdraw (blue) and perceived prices in a specific time-step of the year that was modelled. Under DLMP-based design, Fig. 3(a), in this specific time step, Consumer 4 (C4) seeing a DLMP of 47 euros/MWh is incentivized to inject more, while Consumer 5 (C5) seeing a DLMP of 4 euros/MWh is discouraged from doing so. Additionally, negative network prices prompt larger BESS investments while positive network prices deter BESS investments since greater profit can be made from injecting solar PV power into the grid. The minimal investment in BESS by C4 hints that he is more often subject to positive network prices, compared to the others. Overall, pricing which directly reflects network status encourages significant energy injection (where/when most cost-efficient), driving substantial investments in solar PV as well as optimal BESS investments.

In DOE-based design, consumers are exposed to a common energy price as well as a phase-specific grid capacity price: μ_ϕ . The phase-specific pricing is exemplified in Fig. 3(b). Purchasing grid capacity can serve to (1) provide export capability and (2) amplify import capability. The amount purchased limits the extent to which a consumer may interact with the grid, as delineated in Fig. 3(b) by the thick circle borders confining injection/withdraw. The occurrence of a non-zero grid capacity price indicates that all capacity is, at that time-step, being purchased. According to this price-based allocation dynamic, those consumers with a higher WTP for capacity will secure their desired amount within the bounds of what is available and essentially set the price. This mechanism is evident in Fig. 3(b) among consumers on phase 3. C5 dominates a significant portion of the capacity, leaving consumers 1 and 2 with a minimal amount, where C1 foregoes being a prosumer. A higher WTP for grid capacity corresponds with a higher

⁹ In practice, this signals that we are reaching upper bounds on voltage or branch ratings for upstream power flow.

¹⁰ In practice, this signals that we are reaching lower bounds on voltage or branch ratings for downstream power flow.

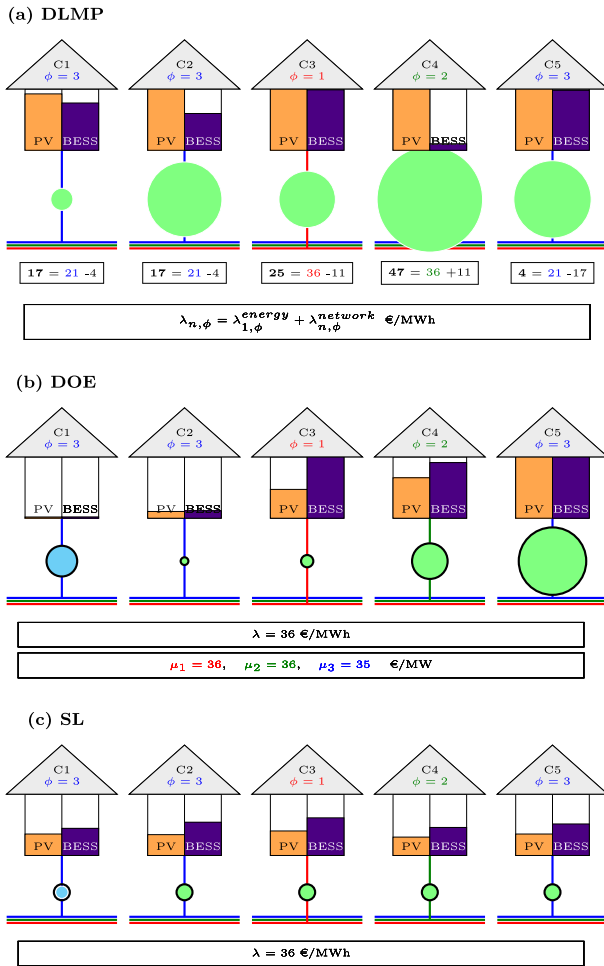


Fig. 3. The three market designs from a consumer perspective. All five consumers are of type small and situated across one network, on varying phases. We showcase their investments in solar PV and BESS using coloured bars as well as their grid interaction for a specific time step using green circles for injection and blue circles for withdraw. Thick circle borders denote a bound on injection/withdraw. The prices observed in each design are stated in boxes.

willingness to install solar PV capacity. Cases in which capacity is scarce and there occur large differences in WTP, result in solar PV capacity being concentrated in the hands of few, potentially leading to a large disparity in installation sizes and injection across consumers, as can be noted in Fig. 3(b).

In SL-based design consumers encounter a common energy price and a static limit on their injection and withdraw capabilities, as delineated in Fig. 3(c) by the thick circle borders. The absence of spatially differentiated price signals, coupled with uniform access to grid capacity, irrespective of location or WTP, results in a homogenization of consumers' ability to interact with the grid. Consequently, consumers face more comparable incentives for installing DER, leading, as shown in Fig. 3(c), to solar PV and BESS installations that resemble each other in size across the consumer base. In contrast to DLMP-based or DOE-based designs, the overall size of these installations tends to be smaller since each consumer need receive an equivalent slice of capacity, discouraging the development of large installations geared towards maximizing profits from injection. What is encouraged, on the other hand, are smaller solar PV assets consistently coupled with BESS in order to avoid curtailment.

6.2. System level outcomes

In the following sections we delve into the comparison of system level outcomes, across the three market designs, considering all 140 cases (14 networks, 10 consumer placements each). We utilize the DLMP-based market design as the benchmark to which we compare the DOE-based and SL-based designs. Therefore, unless specified otherwise, terms such as 'percentage change' and 'percentage point difference', imply the difference from DLMP-based design to simpler design.

The analysis begins with Section 6.2.1 detailing how well simpler designs can approximate the total system cost (TSC), defined in Section 5.3, resulting from a DLMP-based design. How well a simple design can approximate the TSC of DLMP-based design can be directly traced back to how much PCC can be provided, so we detail the factors affecting PCC magnitude in Section 6.2.2 and remind the reader that a definition of PCC can be found in Section 5.2. The factors defining PCC, have consequences on how consumers size their solar PV installations (Section 6.2.3), and subsequently how much total solar PV capacity is installed (Section 6.2.4). Concurrently to solar PV, consumers, driven by price arbitrage opportunities, invest in BESS installations which define how much total BESS capacity is integrated in the system (Section 6.2.5). Simpler designs systematically integrate less solar PV than DLMP-based design. This foregone capacity is replaced with investments in large scale generation technologies, that can supersede those made in DLMP-based design based on how much BESS capacity is installed. This trade-off and its ramifications on the cost efficiency of the generation mix is discussed in Section 6.2.6. The generation mix evidently has an effect on how demand is met (Section 6.2.7) which further defines prices discussed in Sections 6.2.8 and 6.2.9. Finally, the operational decisions defining prices and investment decisions explain consumer costs, discussed in Section 6.2.10.

6.2.1. TSC varies $\leq 1\%$ across market designs

Findings indicate that simpler designs can closely approximate the TSC, defined in Section 5.3, of DLMP-based design. This approximation is less robust under DOE-based design. Additionally, applying a static limit can be more economically efficient than pricing grid capacity.

Across all examined cases, simpler market designs can approximate the TSC of a DLMP-based market design within roughly a 1% increase, as can be seen in Fig. 4(a)–(b). The ability of a simpler design to approximate the TSC of DLMP-based design depends on the network type. The sloping trend, in Fig. 4(a)–(b), indicates that as the PCC decreases, simpler market designs deviate more from approximating the TSC of DLMP-based design. Lower PCC values typically correlate with networks featuring a higher CTDI, *i.e.* networks with longer feeders and greater proportion of small consumers.

In cases offering a high PCC, typically observed in networks with low CTDI (shorter feeders, more condominiums), the DOE-based design closely aligns with the TSC of DLMP-based design, as exemplified in Fig. 4(b). The TSC increase from DLMP-based to DOE-based design in these networks can be as minimal as 0.03%. However, PCC values in DOE-based design exhibit less consistency with varying consumer placement compared to SL-based design, resulting in greater variability in the percentage increase in TSC for the same network. Specifically, this variability is more pronounced in networks with lower CTDI, as evidenced by the blue dots in Fig. 4(b). This implies that the DOE-based design's approximation of DLMP-based design's TSC is more contingent on the demographics of grid users and their locations compared to the SL-based design.

When directly comparing the SL-based with DOE-based design, the latter does not consistently outperform the former in TSC. Across all examined cases, if the PCC in the DOE-based design is 65% or less compared that in SL-based design, applying the latter design will ensure a lower TSC, as can be seen in Fig. 4(c) which illustrates the percentage change in TSC between SL-based and DOE-based design as a function of the percentage change in PCC. In all cases, the DOE-based design

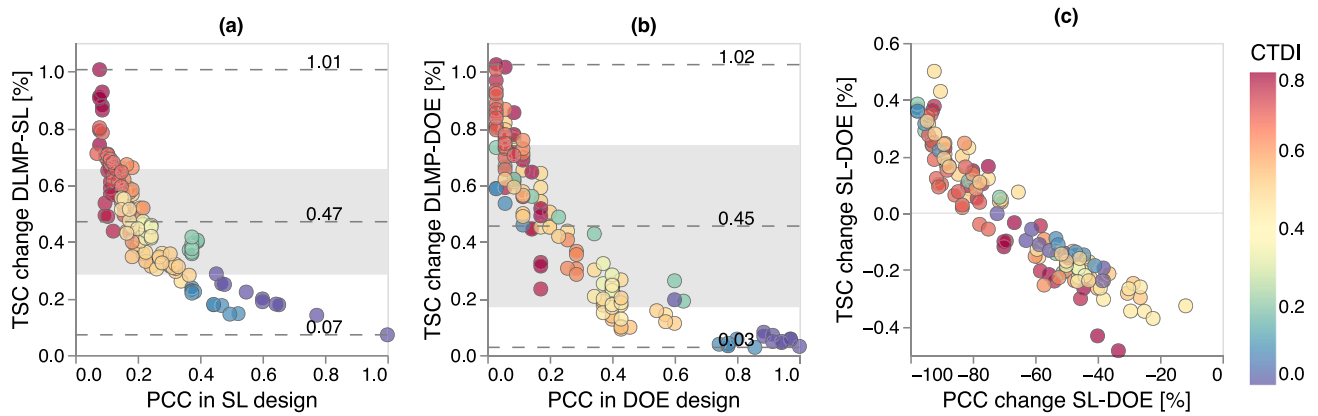


Fig. 4. Panels (a) and (b) illustrate the percentage change in total system cost (TSC), from DLMP-based to simpler design, as a function of the PCC in simpler design. Dashed lines represent maximum, mean and minimum, while shaded region represents standard deviation. Panel (c) illustrates the percentage change in TSC between SL and DOE-based designs as a function of the percentage change in PCC between the two designs. Point colour denotes the CTDI of a network.

consistently offers a lower PCC compared to the SL-based design. This is attributed to the tendency of consumers with a high WTP for grid capacity to exacerbate grid issues.

Overall, the magnitude of PCC plays a pivotal role in determining TSC both across and within market designs. Therefore, we delve into the factors influencing the magnitude of PCC in the following section.

6.2.2. Feeder length, distribution of grid capacity and consumer location influence PCC

Feeder length, how grid capacity is distributed among consumers and the location of consumers with high WTP for grid capacity are the three main factors affecting PCC levels (definition in Section 5.2) and subsequently TSC. Fig. 5 comprises four panels, each illustrating a network at a specific snapshot in time—the time-step in the year where we observe the highest voltage levels due to abundant solar power and injection. DOE-based design and SL-based design are compared under two consumer placements. The first placement allows for more PCC than the second placement. This provides a visual comparison of the network, in simpler designs, under what we term a favourable consumer placement and an unfavourable one.

Networks with a higher CTDI, such as the one depicted, can support only a fraction of the PCC compared to networks with lower CTDI. This limitation arises due to the challenge of maintaining statutory voltage levels at the ends of long feeders when consumers invest in solar PV. Fig. 5 illustrates that voltage levels consistently peak along the longer feeder, potentially reaching upper voltage bounds even when PCC is limited. The reduced PCC in networks with high CTDI leads to a diminished injection of cheap renewable energy (as we will see in Section 6.2.7), resulting in a greater discrepancy in social welfare between the simpler design and DLMP-based design, which, through the use of locational price signals, can successfully manage the congestion that would otherwise trigger voltage magnitude violations. On top of feeder length or, more generally, type of network under consideration, market design can also affect the amount of PCC that can be provided. This is because ensuring network integrity via capacity limits or pricing of grid capacity has ramifications on how grid capacity is distributed and subsequently how consumers interact with the grid. When grid capacity is priced, those with higher WTP will take up their desired amount, which may be relatively large. On the other hand, capacity limits guarantee a homogeneous distribution of capacity. This is visible in Fig. 5, by comparing panels (b) and (d), showcasing DOE-based design, where few are injecting, vs. panels (a) and (c), showcasing SL-based design, where many are injecting similar amounts of power.

Under DOE-based design, one or few consumers, can undermine others' opportunity to inject power, to the detriment of the entire system, as reflected by the TSC of favourable vs. unfavourable placement

in Fig. 5(b) and (d). When one or more consumers with high WTP for grid capacity are situated in network locations prone to violating network limits, this leads to high prices and low PCC to ensure that network limits are respected. This outcome is showcased in Fig. 5(d), in which the PCC is minimal, signifying high grid capacity prices. Overall, this links back to the discussion in Section 6.2.1: what renders the amount of PCC provided in DOE-based design more volatile than SL-based design to consumer placement? It is specifically the location of consumers with high WTP for grid capacity. In turn, this has direct consequences on how robustly DOE-based design can approximate the TSC of DLMP-based design.

The magnitude of PCC and consumers ability to interact with the grid are key factors influencing how they invest in DER, particularly for solar PV. We begin to dissect this in the following section.

6.2.3. Market design impacts solar PV sizing

As can be seen from Fig. 6, which illustrates consumer solar PV and BESS investments for one feeder under two different consumer placements, the DLMP-based design motivates several large solar PV installations. The locational signal efficiently guides consumer interactions with the grid and is therefore conducive to the development of larger, optimally located solar PV investments. Conversely, the SL-based design motivates many, smaller, similarly sized solar PV installations. The static, network-wide limit, imposes a threshold beyond which larger installations are, in absence of the benefit derived from injection, obsolete. In DOE-based design, we note that the nature of solar PV investments is characterized by consumers' WTP for grid capacity, due to this, a larger variance in installation size can arise. In the event of an unfavourable consumer placement, *i.e.* agents with a high WTP for grid capacity located in areas prone to breaching network limits, high grid capacity prices (low PCC) significantly deter solar PV investments. This is evident from the comparison of consumer placement one and four under DOE-based design in Fig. 6.

Additionally, we note a systematic difference in the number of solar PV installations between SL and DLMP-based design. The total number of solar PV installations is always greater in SL-based design than DLMP-based design, in other words, the simpler design motivates a more distributed approach to solar PV investments. This can be seen in Fig. 7(a) which shows the difference in number of installations for all networks and consumer placements as well as the percentage difference in total installed solar PV capacity as a function of PCC. As evident from Fig. 7(a) the siting and sizing of individual solar PV installations has ramifications on the total amount of solar PV capacity present in the system (and consequently TSC), we explore this in the following section.

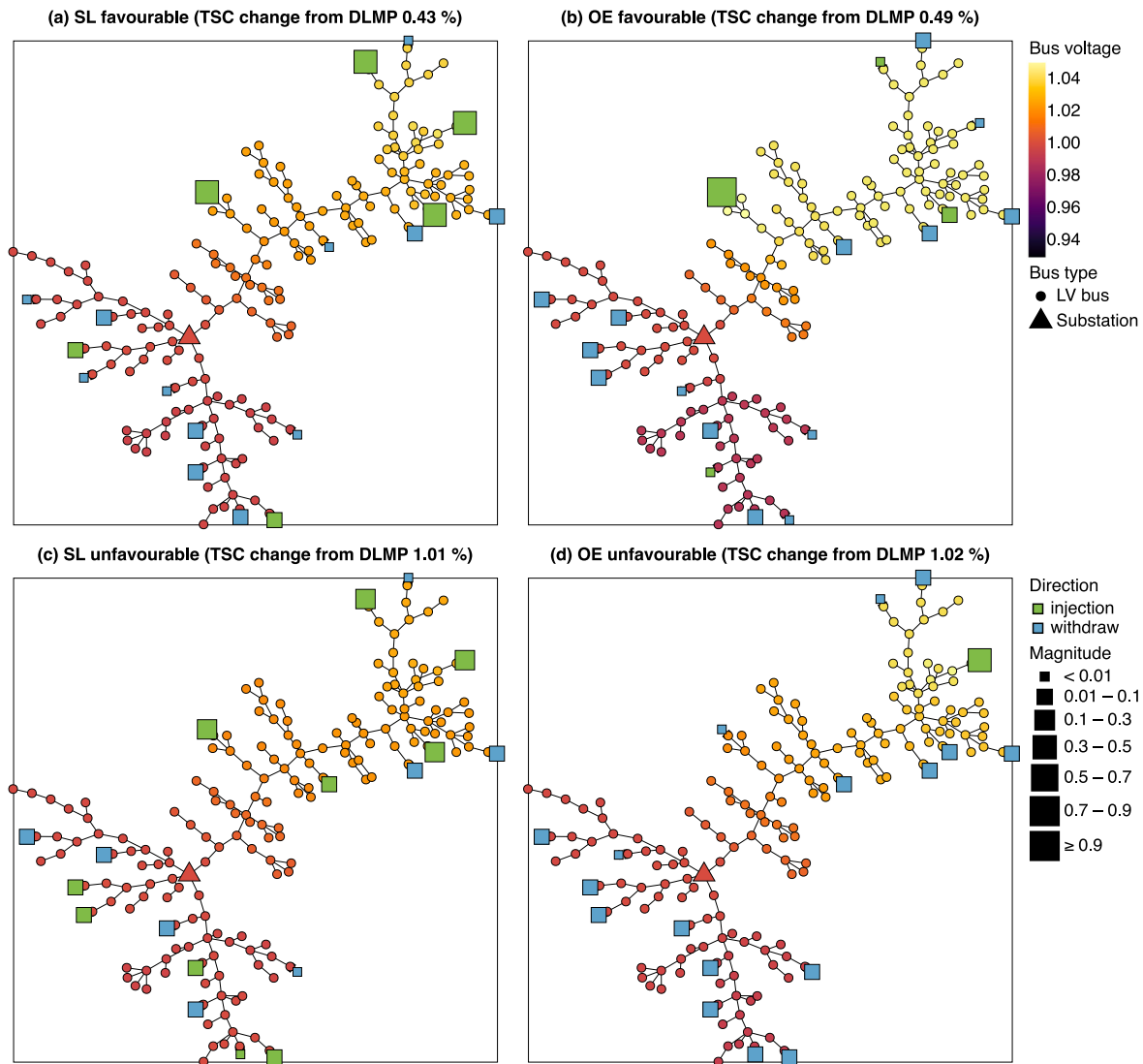


Fig. 5. Network with CTDI 0.79, at time step with highest recorded voltages on phase a, under simpler designs for favourable and unfavourable consumer placements. Lines represent network branches, circles represent network nodes and squares denote consumers (only those on phase a depicted). Node colour indicates voltage magnitude, square colour indicates whether the consumer is injecting or withdrawing and square size denotes the magnitude of the grid interaction. The latter is normalized to the range 0–1 using the largest observed grid interaction.

6.2.4. The DLMP fosters greater solar PV capacity

The larger, strategically placed installations incentivized by the DLMP lead to a consistently higher total solar PV capacity. On average across all cases, SL-based design integrates 35% less while DOE-based design integrates 54% less solar PV capacity compared to DLMP-based design, Fig. 7. Additionally, the higher the CTDI of a network, the lower the PCC and the larger the decrease in solar PV capacity with respect to DLMP-based design. While the locational signal supports efficient operations in these more congestion-prone networks, the lower PCC under simpler designs decreases consumer's ability to inject into the grid, stifling the monetary benefit of owning solar PV and therefore discouraging investment.¹¹ When relating this trend back to Fig. 4,

¹¹ We highlight that a small difference in PCC, occurring, for example, between different consumer locations within the same network, does not mean that, in absolute terms, less solar PV will be integrated. This can be seen in Fig. 6. However, the relative difference between simpler design and DLMP-based design is sustained, since a lower PCC is indicative of greater congestion, which can be better dealt with using a locational signal.

we note that a reduction in solar PV capacity, with respect to DLMP-based design, mirrors the percentage increase in TSC. Besides solar PV, consumers can also invest in BESS. We explore the mechanisms driving the differences in BESS investments in the following section.

6.2.5. Simpler designs yield more distributed BESS

For the majority of cases in DOE-based design and all cases in SL-based design, there is a greater number of BESS installations than in DLMP-based design, as can be seen in Fig. 7(b) which depicts the difference in number of BESS installations for all networks and consumer placements as well as the percentage difference in total installed BESS capacity as a function of PCC. In practice, this means that DLMP-based design motivates a more centralized form of storage, allowing for efficient management and control of energy flow while DOE and SL-based designs motivate a more distributed energy storage model. This is, to a certain extent, also reflected in Fig. 6, wherein we see more, small installations arise in simpler designs. For SL-based design, this, in combination with the fact that also solar PV capacity is more distributed (Section 6.2.3), highlights that consumer's strategy is one with greater focus on self-consumption.

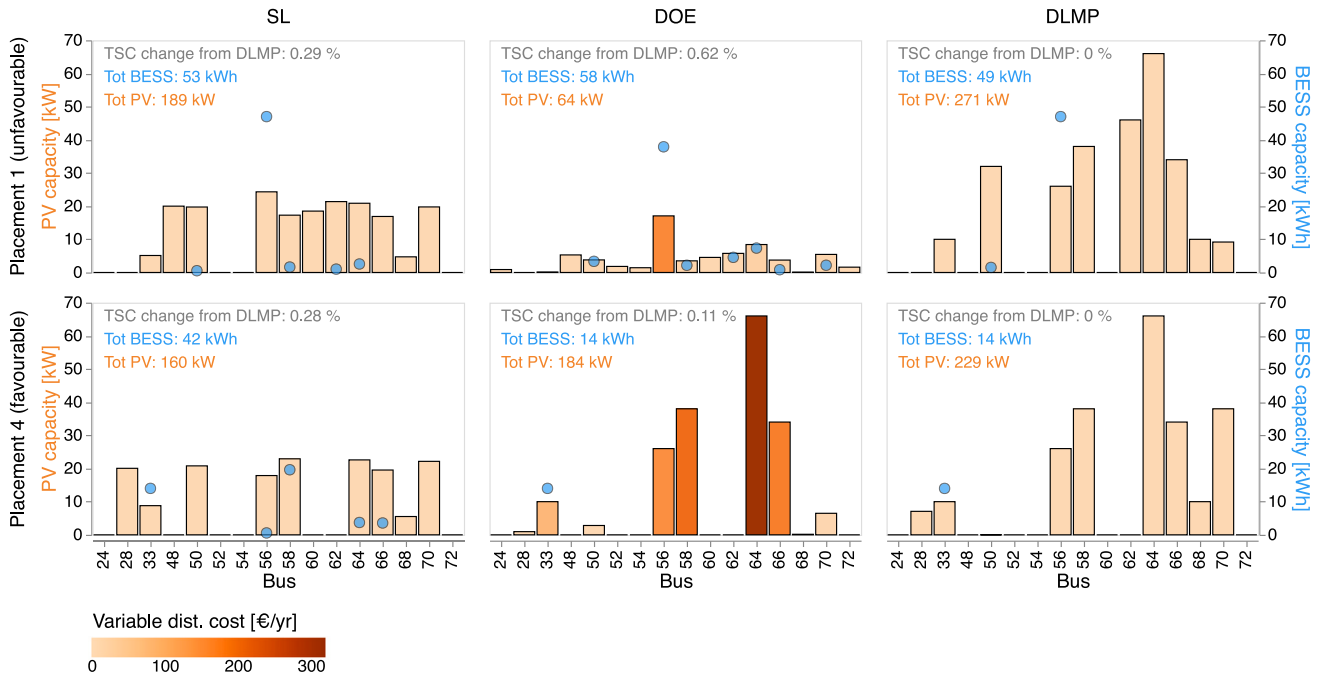


Fig. 6. Capacity of BESS and solar PV installations for consumers on a feeder within network with CTDI 0.51, under the three market designs, two consumer placements. Bar colour represents consumers' variable distribution cost, this is zero in SL-based design and close to zero in DLMP-based design (due to the fact that consumers both pay and are remunerated based on network price component of DLMP). In DOE-based design the variable distribution cost is equivalent to how much consumers spend on grid capacity in the year.

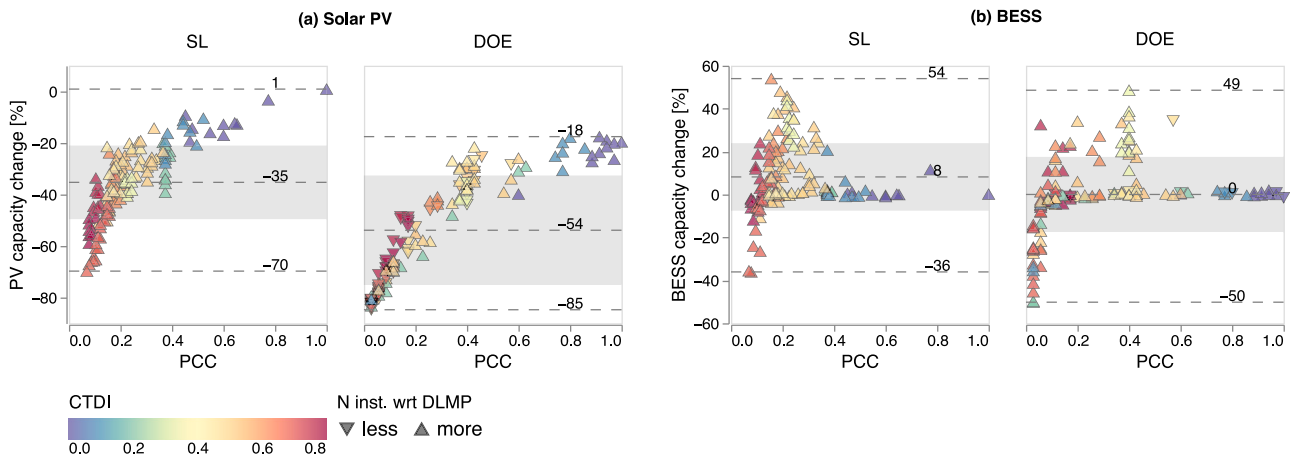


Fig. 7. Percentage change in total installed solar PV capacity (a) and BESS capacity (b) from DLMP-based design for SL-based and DOE-based design. Triangle direction indicates whether simpler design incorporates more or less installations with respect to DLMP-based design. Dashed lines represent minimum, mean and maximum while shaded regions represent standard deviation.

Albeit the larger number of installations in simpler designs, Fig. 7(b), greater total BESS capacity integration is not methodically fostered. The primary driver for BESS investment is the opportunity for price arbitrage, such results indicate that no market design offers a significantly greater opportunity than the others.

Unlike solar PV, it is not straightforward to directly correlate the relative BESS capacity of simpler designs with how accurately they approximate the TSC of DLMP-based design. Rather, we need to consider the interplay between solar PV, BESS and large-scale generator investments. We do so in the following section. We reiterate that in our study, decisions made at the distribution level affect decisions made at transmission level and vice versa.

6.2.6. Technology trade-offs affect cost efficiency

Simpler designs exhibit lower solar PV integration and higher TSC than DLMP-based design. The relative difference in TSC is not excessively elevated due, in part, to the similar levels of conventional generation capacity required by all designs. The variation in TSC across all considered cases arises from the differing approaches in managing reduced solar PV capacity compared to DLMP-based design; substituting it with increased BESS and conventional generation capacity significantly escalates TSC. In Fig. 8, we illustrate the percentage change in conventional generation capacity as a function of the percentage change in total installed BESS capacity. In Fig. 8(a) the colour code denotes relative wind capacity, with respect to DLMP-based design, while in Fig. 8(b) it denotes percentage change in TSC.

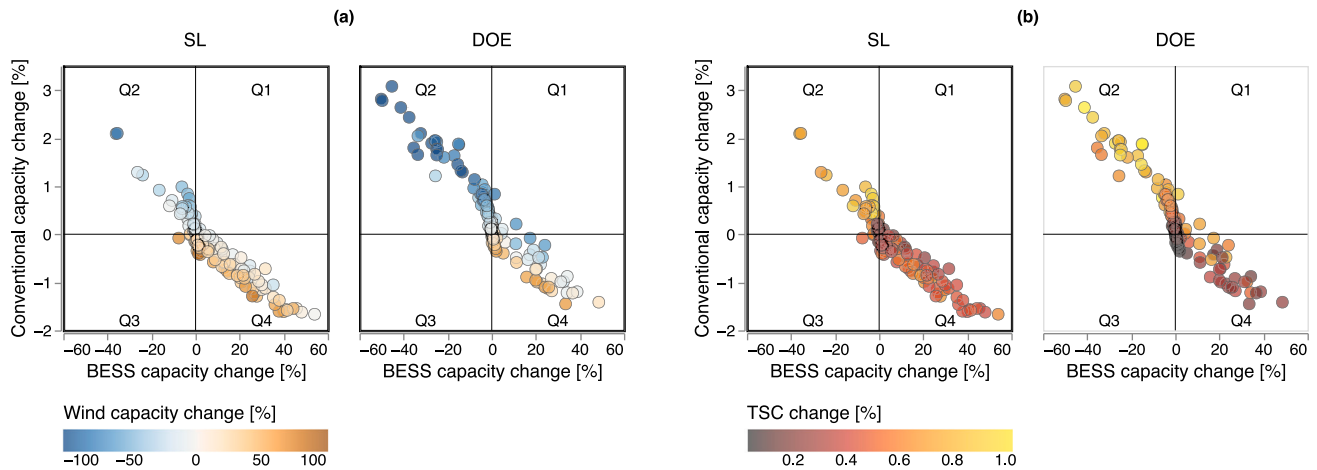


Fig. 8. Percentage change in total installed conventional generator capacity (from DLMP-based to simpler design) as a function of percentage change in total installed BESS capacity (from DLMP-based to simpler design). In (a) colour scale denotes the percentage change in wind capacity and in (b) it denotes the percentage change in TSC, as always, from DLMP-based to simpler design.

While simpler market designs systematically install less solar PV capacity compared to DLMP-based design, conventional generation capacity remains comparable across all market designs. This can be seen from the narrow y-axis range of Fig. 8. Comparable conventional generation capacity is installed due to extended periods of time without renewable energy generation, surpassing storage capacities. Regardless of the solar PV capacity installed, comparable levels of conventional generation capacity are required, across designs, to meet demand during these periods lacking renewable energy generation.

Although no systematic increase or decrease in total BESS capacity was noted between DLMP-based design and simpler designs (Section 6.2.5), there occurs a direct substitution between conventional capacity and BESS capacity between DLMP-based design and simpler designs, as evidenced by the linear relation in Fig. 8. Effectively, in simpler designs, an x% increase in BESS capacity relative to DLMP-based design, driven by greater price arbitrage opportunities, results in a y% decrease in conventional capacity, again relative to DLMP-based design. Simultaneously, greater BESS capacity in simpler designs compared to DLMP-based design is synonymous with increased wind penetration, as can be seen from the colour scale in Fig. 8(a).

In terms of TSC, cases with conventional and BESS capacities closest to DLMP-based design best approximate its TSC. In moving further from the origin in any direction, the approximation of the DLMP-based design’s TSC worsens, albeit to varying extents. Cases with less conventional capacity, more BESS, and more wind (Q4) are less cost-efficient, while the most cost-inefficient cases are those with more conventional capacity, less BESS, and less wind (Q2). This can be seen from the colour scale of data points, in Fig. 8(b).

This trend can be linked back to the CTDI of a network. In increasing CTDI, synonymous with decreasing PCC, networks are unable to integrate as much solar PV capacity as in DLMP-based design. Albeit resulting in a less cost-efficient system, the system makes up for the loss in solar PV with additional BESS and wind capacity, displacing conventional generation capacity, relative to DLMP-based design (Q4). When CTDI increases even further, and PCC decreases, networks under simpler designs can only integrate a small fraction of solar PV capacity compared to that in DLMP-based design. With little solar PV in the system, the incentive for BESS investments, or price arbitrage opportunity, also decreases, such that the system replaces missing solar PV capacity with conventional generation capacity, foregoing BESS as well as wind farm investments, leading to the most cost-inefficient systems (Q2).

Across market designs, changes in the generation technology mix affect how the system meets demand, we detail how this is so in the next section.

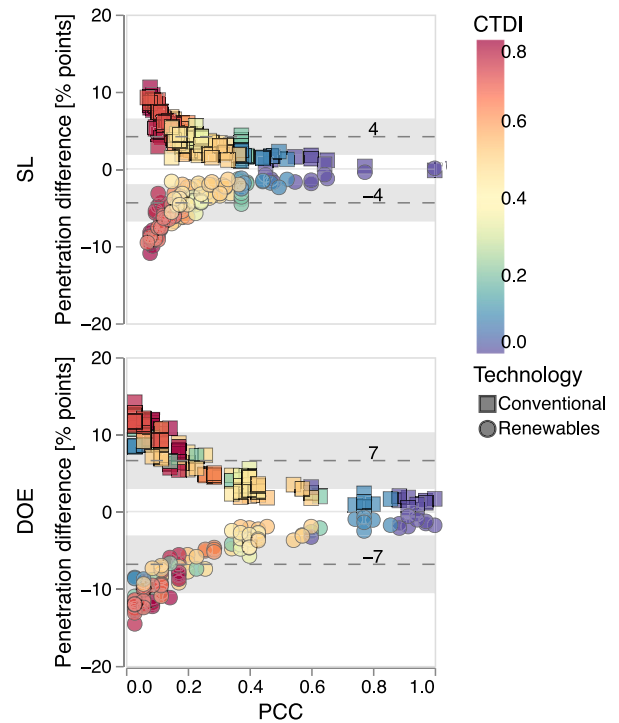


Fig. 9. Percentage point difference between DLMP-based and simpler design in renewable (solar + wind) and conventional penetration as a function of PCC. Penetration is defined as the portion of demand that can be satisfied from generation from respective technologies. Dashed lines represent mean and shaded regions represent standard deviation.

6.2.7. Simpler designs rely more on conventional generation

Compared to DLMP-based design, in simpler market designs, a lower portion of demand is satisfied by renewable sources such as wind and solar PV, with the latter having a larger impact on this reduction. Under simpler designs, the system is more reliant on generation from conventional resources. This can be seen in Fig. 9 which illustrates the percentage point difference in penetration of generation from conventional technologies and renewable technologies (solar PV and wind) for each simpler market design as a function of PCC.

The trade-off between decreased renewable penetration and increased conventional penetration is exacerbated in networks with higher CTDI. This can be linked back to solar PV capacity, which, as

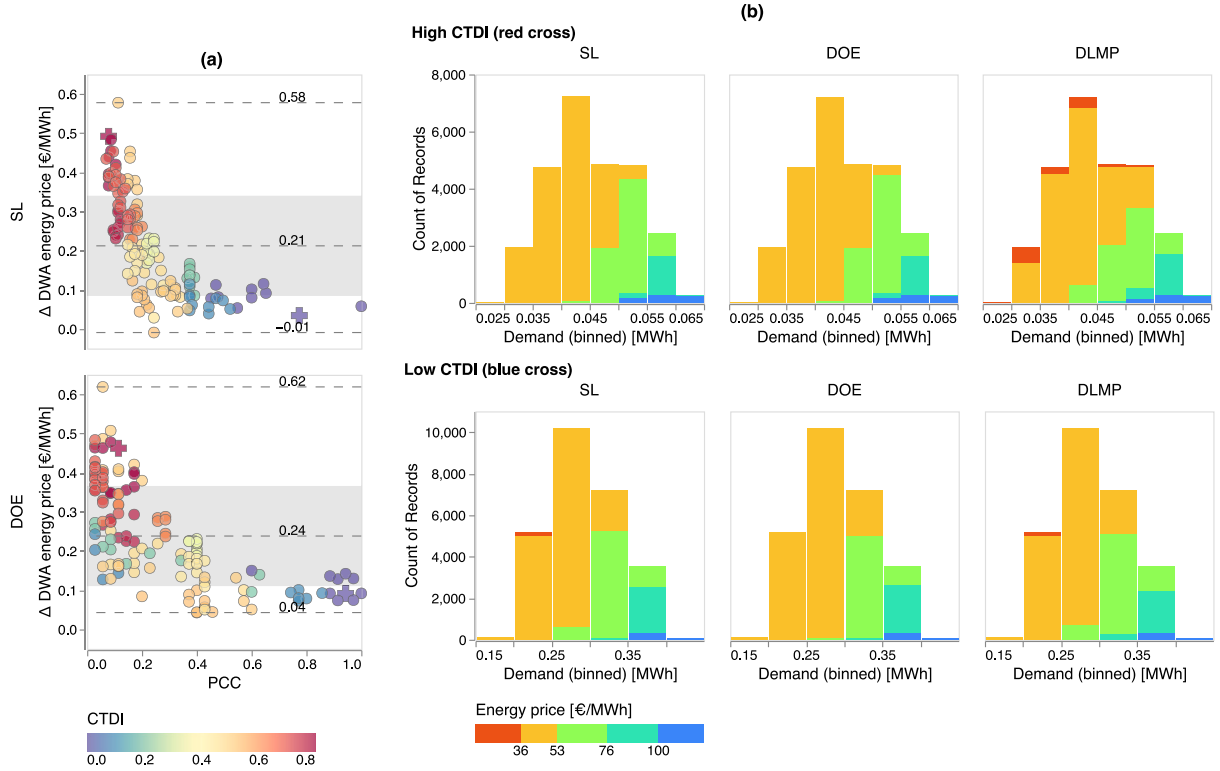


Fig. 10. Panel (a) illustrates the difference in demand weighted average (DWA) energy price. Panel (b) illustrates, for two cases, shown as cross-shaped points in panel (a), the energy prices observed for binned tranches of demand. Colour scale is sub-divided using the variable costs of base (36 EUR/MWh), mid (53 EUR/MWh) and peak-load (76 EUR/MWh) conventional generation technologies.

previously analysed, decreased drastically compared to DLMP-based design for networks with higher CTDI (Section 6.2.4).

Given the very limited PCC in certain cases under DOE-based design, a notable reduction in solar PV capacity compared to DLMP-based design ensues, leading, in turn, to a more pronounced trade-off between increased conventional and diminished renewable penetration compared to SL-based design.

Since the dynamics of how system demand is satisfied differs across the market designs so too do energy prices, having ramifications on the costs borne by consumers. In the next section we address the differences in energy prices.

6.2.8. Simpler designs yield higher average energy prices

In Fig. 10(a), we illustrate the difference in demand weighted average (DWA) energy price between DLMP-based design and simpler designs for all considered cases. The DWA energy price is a measure of the average price of energy, taking into account the variations in energy demand across different time steps.¹² If the DWA energy price is higher for one case compared to another, it indicates that, on average, the cost of energy is higher when considering the demand at each time step. We can distinguish between energy price and network price within a DLMP since the DLMP occurring at the slack node exclusively represents the energy price, whereas at all other nodes it is the sum of energy and network prices. We further show in Fig. 10(b) the energy prices seen per demand level for two particular cases: a network with high CTDI and a network with low CTDI.

¹² Mathematically defined as follows, where dw_t is the day weight:

$$\text{DWA energy price} = \frac{\sum_t \text{Total demand}_t \times dw_t \times \text{energy price}_t}{\sum_t \text{Total demand}_t \times dw_t} \quad (51)$$

The DWA energy price is typically higher under simpler designs compared to DLMP-based design. Furthermore, this difference becomes more pronounced as the CTDI of a network increases, mirroring, as previously seen the relative reduction in solar PV capacity and renewables penetration. Under simpler designs, networks with low CTDI, can better approximate the amount of demand met by solar PV generation in DLMP-based design, consequently resulting in similar operational costs and energy prices. On the other hand, networks with lower CTDI, under simpler designs, only have a fraction of the solar PV generation present in DLMP-based design. As such, in these networks, while DLMP-based can meet a greater portion of demand at prices that fall below the variable cost of base load generator, a simpler design cannot, Fig. 10(b), resulting in a higher DWA energy price. Regardless, we note that this does not yield a largely different average DWA energy price, as the bulk of demand is still, as exhibited in Fig. 10(b), across all designs, met at similar prices.

In DLMP-based and DOE-based design the dynamics of how system demand is satisfied also impacts the network or grid capacity price, which too have ramifications on costs borne by consumers. We detail the network prices seen by consumers under DLMP-based design in the next section. In Appendix F the reader can find further detail on grid capacity prices seen by consumers in DOE-based design.

6.2.9. DLMPs are most beneficial in networks with longer feeders

Across the considered cases, non-zero network prices occur for no more than 25% of the year but can, throughout the year, affect the majority of the network. This can be observed in Fig. 11 (exclusive to DLMP-based design) which, in panel (a) illustrates the frequency of occurrence of network prices in time and space. Non-zero network prices occur especially in networks with higher CTDI. In practice, this means that the infrastructure limits of networks comprising longer feeders, with a greater portion of small consumers, are more readily reached when consumers invest in DER. Implementing a DLMP-based market in

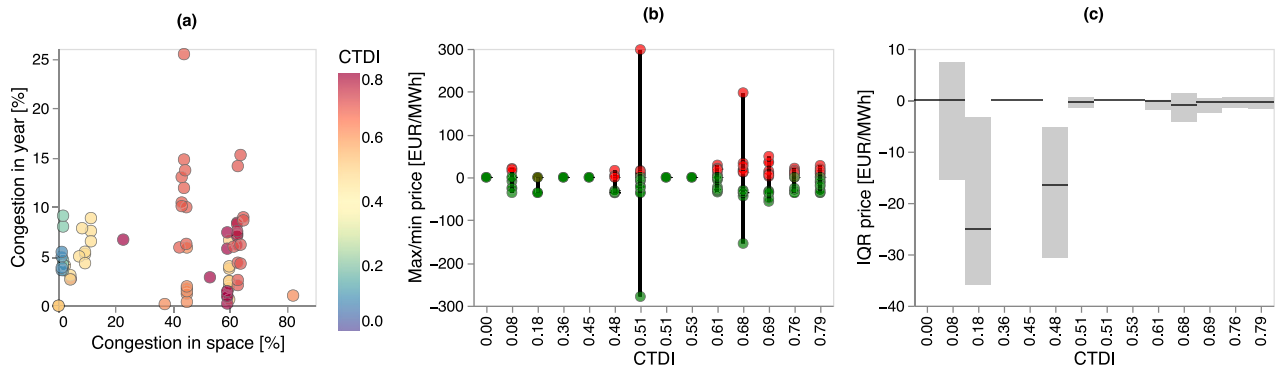


Fig. 11. DLMP-based market network prices. Panel (a) illustrates the occurrence of non-zero network prices throughout the year (*i.e.* the percentage of hours in which there are non-zero network prices) as a function of the occurrence of non-zero network prices in space (*i.e.* the percentage of nodes in the network witnessing non-zero network prices in the year). Panel (b) illustrates maximum (red) and minimum (green) observed network prices per consumer placement, per network, identified via CTDI. Panel (c) illustrates the interquartile range (IQR) of observed non-zero network prices per network, again identified via CTDI. The solid line indicates the median.

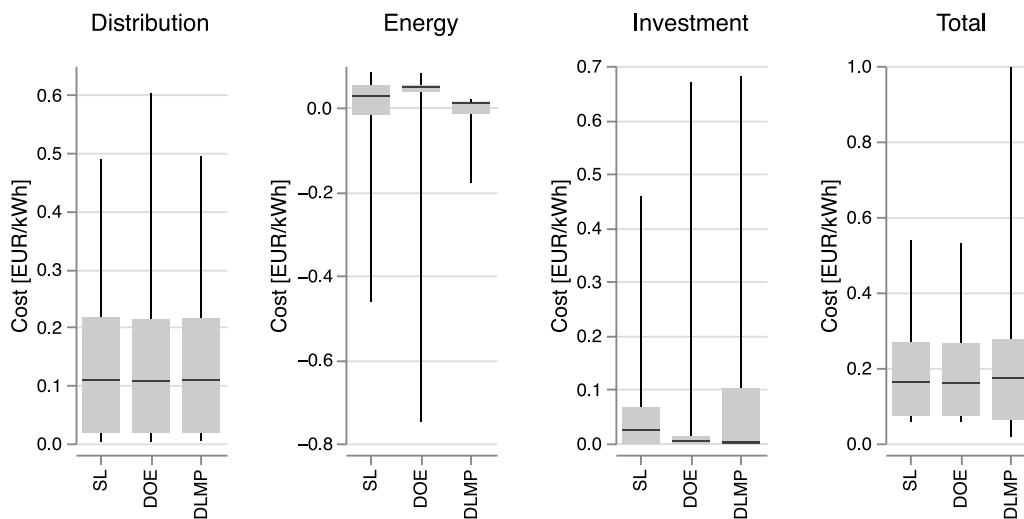


Fig. 12. Yearly consumer costs under each market design. Each box plot encompasses all consumers under all networks and consumer placements. Distribution (fixed + variable), energy, investment and total cost are shown. Each consumers yearly cost is divided by their demand to obtain units of EUR/kWh.

these networks, signalling to consumers the occurrence of congestion can, as seen by the ramifications on TSC (Section 6.2.1), prove more beneficial than in networks with lower CTDI. It is important to note that the locational aspect of DLMPs, means that network prices can differ across the network but even between phases of the same node.

In terms of magnitude, network prices in DLMP-based design can, in our system, range anywhere between 300 EUR/MWh and -280 EUR/MWh as depicted by the network price spreads of Fig. 11(b). However, these are exceptional cases in which the flow of power upstream/downstream surpasses that of a branch power rating, leading to a bottleneck. As shown in Fig. 11(b), maximum and minimum network prices typically oscillate between 50 and -50 EUR/MWh. Fig. 11(c), illustrating the interquartile range (IQR) of network prices per network, indicates that the majority of observed network prices are negative. Signalling that LVDS limits are being reached due to local solar PV generation, *i.e.* power flowing upstream. A negative network price discourages injection from solar PV by reducing the associated monetary benefit, this is a unique ramification that DLMP-based design has on the profits consumers can make. We delve into further detail on this in the next section which reviews all net costs borne by consumers.

6.2.10. Consumers experience comparable total costs across designs

Finally, we analyse the costs borne by consumers in the following section. These costs are: energy costs, DER investment costs and

distribution-related costs. The individual distribution cost for consumers is, in DOE and DLMP-based designs, made up of a variable as well as a fixed component.¹³ Fig. 12 exhibits the distribution, energy and investment costs of all consumers under each design, as well as the total of these three. The cost is normalized against each consumers' demand, thus portrayed as EUR/kWh. We highlight that a consumer's energy cost is the sum of what he pays for withdrawing and receives for injecting power throughout the year.

Distribution costs. Distribution fees are similar across designs. Knowing that in SL-based design all consumers are paying 400 EUR/year, we can say that also in DOE-based and DLMP-based design most consumers, summing both variable and fixed payments, are paying approximately this yearly amount. This indicates that, in total, variable distribution payments are not significant enough to largely offset the fixed distribution payment and that the latter is, in all designs, an essential means for DSO cost recovery.

Few consumers in DOE-based design, however, are subject to higher distribution costs, in absolute terms, the observed maximum is of 770

¹³ We highlight that in DLMP-based design variable distribution payments can be positive or negative, depending on network price and consumer interaction with the grid.

EUR/year. These are consumers with large solar PV assets who can offset this distribution cost by making a profit from injecting energy into the grid.

Energy and investment costs. The comparison of consumers' energy costs between designs reveals that in DLMP-based design, median energy costs are closest to zero, suggesting a central tendency toward lower energy expenses compared to both SL-based and DOE-based design. Additionally, the box plots' spread indicates that, in DLMP-based design, there is lower variability in energy costs across all consumers. In practice, in DLMP-based design, the occurrence of lower energy prices during instances of simultaneous injection prevents consumers from making exceptional profit. Concurrently, significant injection of cheap, solar energy, benefits those consumers who do not own a solar PV asset, leading to greater homogenization of energy costs across consumers. As can be seen from consumers' investment costs, a greater portion of the consumer population is making greater investments in DER, compared to the other two designs.

Median energy costs are highest in DOE-based design, confirming, as previously found, that consumers are subject to higher energy prices than in DLMP-based design. The small, positive IQR suggests that there is very little variability in the majority of consumers' energy costs, pointing to the fact that these consumers do not own solar PV and are relying on withdrawing from the grid. On the other hand, the presence of extreme negative energy costs indicates that there exist few consumers owning significant DER capacity and making substantial profit from injection into the grid, benefitting from the higher energy prices. Overall, this is mirrored in consumers' investment costs, whereby 75% of consumers are investing in little to no DER, while 25% are making significant investments. The operating profits made serve to offset these large investment costs.

In SL-based design, the largest DER investments do not reach the same level as those found in the other two designs. This, albeit similar energy prices to DOE-based design, prevents the occurrence of very negative energy costs for certain consumers. A higher median consumer investment cost is nonetheless observed, as more consumers are making small DER investments, leading to lower median energy costs, than those found in DOE-based design.

Total costs. Total consumer costs across the three designs, for most consumers, are similar, as can be seen by the comparable box plots in the last panel of Fig. 12. Due to the fact that injecting into the grid is not as lucrative in DLMP-based design as it is in the simpler designs, there occur some consumers who, having made large DER investments face larger total costs. Generally however, and although achieved through different mechanisms, similar total costs are borne by the majority of consumers across the three designs. In practice, what occurs is a trade-off between cost components between the designs. In DOE-based design consumers with large solar PV assets are able to offset higher distribution costs and investment costs with significant profits from injection. SL-based design, on the other hand, strikes a balance with modest DER investments and comparatively lower median energy costs. DLMP-based design, with its higher solar PV penetration, yields low energy costs as well as profits, benefitting most with the exception of those having purchased large DER with respect to their demand.

7. Conclusion

Increased accessibility of DERs warrants a paradigm shift in power generation and consumption, with end-use customers in LVDS actively participating in electricity production and storage. Successfully integrating DERs into the electricity market, to fully harness their benefits, however, necessitates effective mechanisms for guiding interactions of self-interested agents with LVDS in order to manage local grid constraints. Static limits (SLs), Dynamic Operating Envelopes (DOEs), and Distribution Locational Marginal Pricing (DLMP) have all been suggested as means to ensure network integrity within the context

of DER market participation. In this paper, we address the trade-off between complexity and economic efficiency of market designs using SLs, DOEs and DLMPs. Highlighting the significance in recognizing the nuances associated with balancing system reliability, economic efficiency, and consumer costs through these different approaches. We systematically compare SLs, DOEs, and DLMPs from a long-run market equilibrium perspective, considering investments in both customer-owned DERs and transmission-level generators. The analysis explores the system-level ramifications of each approach, filling a critical void in the literature that often adopts an operational perspective without factoring in investments and the feedbacks between distribution and higher voltage levels.

Our analysis has shown that simpler market designs, such as SL-based design and DOE-based design, can approximate the economic efficiency of DLMP-based design. However, the proximity of the approximation is dependent upon the type of network under consideration. While simpler designs can closely approximate the economic efficiency of DLMP-based design in networks comprising shorter feeders and larger consumers (at a fraction of the implementation complexity) the same cannot be said for networks comprising longer feeders with many small consumers. The locational signal provides significant added value, in effectively managing congestion, within such networks wherein infrastructure limits are more readily reached in presence of DER. Simpler designs cannot match the benefit of the DLMP by providing ample enough capacity limits or low enough capacity prices that incentivize comparable levels of solar PV investments and injection of cheap, renewable energy into the grid. As a byproduct, systems within simpler designs lead to less cost efficient investments resulting in heavier reliance on generation from conventional technologies.

Additionally, considering consumer preferences in the allocation of DOEs by means of grid capacity pricing has shown that the self-interested behaviour of few actors can significantly undermine others' opportunity to inject, leading to a lower economic efficiency than SL-based design. If consumers with a high willingness to pay (WTP) for grid capacity are located in locations prone to triggering network limit violations the problem can be even further exacerbated. This is also true if there is significant variation in WTP for grid capacity across the consumer base. As such, this renders the DOE-based designs approximation of DLMP-based design's economic efficiency, strongly dependent on the set of consumers using the grid and their location. If the allocation of grid capacity is approached through pricing, careful consideration must be given to the heterogeneity of the consumer base.

While there are important differences at system level, the majority of consumers are subject to comparable yearly total costs across the three designs due to trade-offs between distribution, energy and DER investment costs. For example, in DOE-based design a consumer may pay higher distribution costs and make larger investments, compared to the other two designs, but offset these with profits from injection. The flexibility arising from the fact that consumers experience similar total costs across the three designs means that it is possible to implement diverse designs across different feeders of the same network, especially in cases where applying the DLMP-based design to the entirety of a network may still be impractical. Interestingly, albeit price differentials are inherent to DLMP-based design, a factor that has triggered significant discussion on the fairness of implementing such approach, our study has revealed that this design offers highly harmonized energy costs among the consumer base and total costs, for the majority of consumers, similar to those under simpler designs, with the exception of those making significant investment in DER.

CRedit authorship contribution statement

Chiara Gorrasi: Writing – review & editing, Writing – original draft, Visualization, Methodology, Formal analysis, Data curation, Conceptualization. **Kenneth Bruninx:** Writing – review & editing, Supervision, Conceptualization. **Erik Delarue:** Writing – review & editing, Supervision, Funding acquisition.

Declaration of competing interest

The authors declare that they have no known competing financial interests or personal relationships that could have appeared to influence the work reported in this paper.

Data availability

Data will be made available on request.

Acknowledgements

This work was supported by the Belgian Federal Energy Transition Fund, via the Bregilab project.

Appendix A. Branch rating constraints

Branch rating constraints, also referred to as thermal limit constraints, are designed to prevent the power flowing through a branch from surpassing its apparent power rating. Conventionally, these constraints are expressed by ensuring that the squares of the active power, $p_{t,l,\phi}^{flow}$, and reactive power, $q_{t,l,\phi}^{flow}$, flowing through the branch remain below the square of the apparent power rating of the branch $\bar{S}_{l,\phi}$. Geometrically this represents a circle. To express these constraints in a linear form, we utilize the following procedure to create an inner approximation of the circle using a polygon:

1. Set the maximum gap (gap^{max}), relative to the circumference of the unit circle, between consecutive points on the circle. A value of 0.04 means that the gap between points is approximately 4% of the circumference of the circle.
2. Use (52) to calculate the number of points N needed to create the inner approximation.
3. Use (53) to calculate N complex numbers evenly spaced around the unit circle, and scale them by the power rating of the branch ($\bar{S}_{l,\phi}$). This represents the linear approximation of the circle.
4. Implement a cyclic rotation of the elements in the linear approximation vector, as shown in (54). This rotation operation helps in forming a more diverse set of points and contributes to the creation of a dodecahedron.
5. Take the average of each pair of corresponding complex numbers from the linear approximation and its rotated version, as described in (55). This ensures that the resulting complex numbers are evenly distributed between the original linear approximation and its rotated version.
6. Finally, use the real A and imaginary B parts of the complex numbers in \mathbf{D} in the branch rating constraints (56). This results in 12 lines, these twelve lines form a dodecahedron inside the original circle.

$$N = \lceil \frac{\pi}{\arccos(1 - gap^{max})} \rceil \quad (52)$$

$$\mathbf{a} = \begin{bmatrix} \bar{S} \cdot \left(\exp\left(\frac{i \cdot 0 \cdot 2\pi}{N}\right) \right) \\ \bar{S} \cdot \left(\exp\left(\frac{i \cdot 1 \cdot 2\pi}{N}\right) \right) \\ \vdots \\ \bar{S} \cdot \left(\exp\left(\frac{i \cdot (N-1) \cdot 2\pi}{N}\right) \right) \end{bmatrix} \quad (53)$$

$$\mathbf{a}^{rot} = \begin{bmatrix} \mathbf{a}[N] \\ \mathbf{a}[1] \\ \vdots \\ \mathbf{a}[N-1] \end{bmatrix} \quad (54)$$

$$\mathbf{D} = \frac{1}{2} (\mathbf{a} + \mathbf{a}^{rot})$$

$$\begin{aligned} &= \frac{1}{2} \left(\begin{bmatrix} \mathbf{a}[N] \\ \mathbf{a}[1] \\ \vdots \\ \mathbf{a}[N-1] \end{bmatrix} + \begin{bmatrix} \mathbf{a}[1] \\ \mathbf{a}[2] \\ \vdots \\ \mathbf{a}[N] \end{bmatrix} \right) \\ &= \frac{1}{2} \begin{bmatrix} \frac{\mathbf{a}[N]}{2} + \frac{\mathbf{a}[1]}{2} \\ \frac{\mathbf{a}[1]}{2} + \frac{\mathbf{a}[2]}{2} \\ \vdots \\ \frac{\mathbf{a}[N-1]}{2} + \frac{\mathbf{a}[N]}{2} \end{bmatrix} \\ &= \begin{bmatrix} A_1 + B_1 \cdot i \\ A_2 + B_2 \cdot i \\ \vdots \\ A_N + B_N \cdot i \end{bmatrix} \end{aligned} \quad (55)$$

$$A \cdot p_{t,l,\phi}^{flow} + B \cdot q_{t,l,\phi}^{flow} \leq A^2 + B^2 \quad (56)$$

$$\forall t \in \mathcal{T}, (A, B) \in \mathbf{D}, l \in \mathcal{L}, \phi \in \Phi$$

Appendix B. EOP formulation

The objective function for EOP_{DOE} and EOP_{SL} is the same, as shown in (57), while EOP_{DLMP}'s objective differs due to the inclusion of penalty terms aimed at promoting convergence, as depicted in (58). Each EOP encompasses a set of constraints, with many of these being common across market designs. These constraints pertain to consumer DER operation (4)–(20), conventional generator operation (32)–(35), and renewable generator operation (37)–(38). However, constraints related to consumer-grid interaction and those governed by the network-aware market operator vary across designs. The presence of these constraints in each EOP is detailed in Table 3.

$$\begin{aligned} \boxed{\text{SL}}, \boxed{\text{DOE}} \min & \sum_{g \in \mathcal{G}} \left(\sum_{t \in \mathcal{T}} \sum_{\phi \in \Phi} (VC_g^P \cdot pc_{g,t,\phi} + VC_g^Q \cdot qc_{g,t,\phi}) \right) \\ & + IC_g^C \cdot cap_g^C + IC^W \cdot cap^W + \sum_{j \in \mathcal{J}} \left(IC_j^{PV} \cdot cap_j^{PV} \right. \\ & \left. + IC_j^{PVi} \cdot cap_j^{PVi} + IC_j^S \cdot cap_j^S + IC_j^{Si} \cdot cap_j^{Si} \right) \end{aligned} \quad (57)$$

$$\begin{aligned} \boxed{\text{DLMP}} \min & \sum_{g \in \mathcal{G}} \left(\sum_{t \in \mathcal{T}} \sum_{\phi \in \Phi} (VC_g^P \cdot pc_{g,t,\phi} + VC_g^Q \cdot qc_{g,t,\phi}) \right) \\ & + IC_g^C \cdot cap_g^C + IC^W \cdot cap^W + \sum_{j \in \mathcal{J}} \left(IC_j^{PV} \cdot cap_j^{PV} \right. \\ & \left. + IC_j^{PVi} \cdot cap_j^{PVi} + IC_j^S \cdot cap_j^S + IC_j^{Si} \cdot cap_j^{Si} \right) \\ & + P_{pen} + Q_{pen} \end{aligned} \quad (58)$$

Table 3

Constraints specific to each market design in the EOP formulation. The abbreviation FBS is for FBSUBFPowerModel, signalling that EOP_{DLMP} encompasses all constraints pertaining to this power flow formulation within the *PowerModelsDistribution.jl* package.

Agent	EOP _{SL}	EOP _{DOE}	EOP _{DLMP}
Consumer	(21)–(24)	(25)–(29)	–
Market op.	(39)–(40)	(39)–(40), (41)	(56), FBS

Appendix C. Learning curve method

The 2019 solar PV costs sourced from [52] are as shown in Table 4. According to [58] we apply a learning curve (LC) of 0.89 for balance of system (BOS) as well as inverter costs and one of 0.80 for module costs. Using capacity projections found in [59], we then apply (59) and (60) to derive 2030 costs. We find the 2030 total solar PV system cost to be 577 €/kW, breaking this down into module/panel, plus BOS cost, of 481 €/kW and inverter cost of 96 €/kW.

$$LC = 2^{-\beta} \quad (59)$$

$$Cost_{2030} = Cost_{2019} \times \left(\frac{Capacity_{2030}}{Capacity_{2019}} \right)^{\beta} \quad (60)$$

Table 4

Costs for solar PV installations.
Source: Sourced from [52].

System component	Cost 2019 [€/W]
Module	0.36
Inverter	0.22
BOS	0.68

Appendix D. Network data

In Table 6 we provide further information on the utilized networks: the ID of the network, CTDI, the number of nodes, branches, feeders, overall length, the total number of households, the number of condominiums, individual houses and other loads present in the network.

Appendix E. Computational complexity

The equivalent optimization problems (EOPs) used to find a Nash equilibrium in each market design, were implemented in Julia [60] using JuMP [61] with the solver Gurobi [62]. For the AC power flow simulation (performed to check whether the chosen Ω leads to a network admissible solution in SL and DOE-based designs) the solver Ipopt [63] was used. All optimizations/simulations were run on a Macbook Pro with Apple M1 Pro chip and 16 GB RAM. For each market design the average computation time and number of iterations, across all considered networks and consumer placements (140 cases) are shown in Table 5. As it entails an explicit power flow model, the EOP_{DLMP} does not need an ex-post power flow simulation to check for network feasibility of the solution. On the other hand, EOP_{DOE} and EOP_{SL} do since instead of power flow constraints they rely on an exogenously set Ω to ensure a network admissible solution. As such, for DOE-based and SL-based designs EOP and AC simulation are run sequentially, starting from an Ω of zero up until the magnitude of Ω is found to cause network issues such as over/under voltage or exceeding branch ratings, using a step-size of 0.01 kW for Ω . Iterations of EOP_{DLMP} are required to find an AC-admissible solution based upon the successive approximation approach involving linearized power flow constraints.

Table 5

Average computation time in seconds and number of iterations for each market design, across all considered networks and consumer placements.

Design	Solve EOP [s]	AC simulation [s]	Iterations
DLMP	62	n/a	5.6
DOE	17	35	0– Ω
SL	12	33	0– Ω

Table 6

Network information.

ID	CTDI	Nodes	Branches	Feeders	Length [m]	Households	Condominiums	Houses	Other loads
65019	0.68	248	247	6	3041	351	23	47	23
65025	0.36	307	306	6	3346	308	42	23	60
65068	0.08	180	179	9	2603	591	39	3	30
65016	0.61	129	128	2	1837	135	16	19	18
65028	0.69	207	206	4	3819	233	21	39	28
65043	0	83	82	5	1450	429	24	0	31
65031	0.45	124	123	4	1598	135	16	13	21
1830188	0.19	127	126	5	2171	371	23	5	24
1142831	0.76	163	162	4	2514	98	11	33	21
1459343	0.79	181	180	5	3445	68	8	36	5
1351982	0.48	97	96	4	1290	111	9	10	20
1132967	0.53	190	189	8	2678	232	22	27	22
1136065	0.51	179	178	5	2968	166	8	52	14
86315	0.51	143	142	6	2676	319	22	12	17

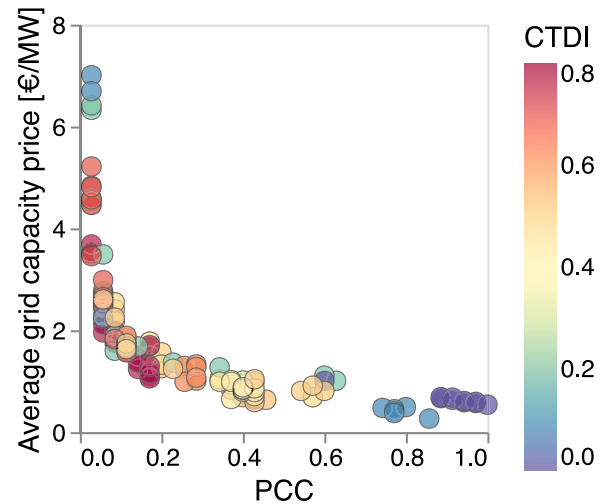


Fig. 13. Yearly average grid capacity prices in DOE-based design as a function of PCC. The unit of grid capacity price is €/MW but can also be €/MWh in our specific case since the market is cleared hourly.

Appendix F. Grid capacity prices

In DOE-based design, consumers can purchase grid capacity to export power to the grid or to augment their import capabilities. Fig. 13 depicts the yearly average grid capacity price of each case as a function of PCC. The sloping trend indicates that the lower the PCC the higher the average cost of grid capacity. Under DOE-based design, as seen throughout previous analysis, the interrelation between higher CTDI and lower PCC is not as strong as in SL-based design. This is because unfavourable consumer placements under DOE-based design can significantly restrict the amount of PCC. As such, even networks with high CTDI can, at times, present high grid capacity prices. Playing into the magnitude of these prices is also the relative WTP of consumers within each case, the stronger the competition the higher the price.

References

- [1] Franklin E, Alam KS, Amin M, Negnevitsky M, Scott P, Iria J, et al. Optimal DER scheduling for frequency stability. Technical report, University of Tasmania & Australian National University; 2022, Available at: https://www.researchgate.net/profile/Jose-Iria-2/publication/359434837_Optimal_DER_Scheduling_for_Frequency_Stability_Study_Report/links/624542a35e2f8c7a034adbed/Optimal-DER-Scheduling-for-Frequency-Stability-Study-Report.pdf.
- [2] Neetzow P, Mendelevitch R, Siddiqui S. Modeling coordination between renewables and grid: Policies to mitigate distribution grid constraints using

- residential PV-battery systems. *Energy Policy* 2019;132:1017–33. <http://dx.doi.org/10.1016/j.enpol.2019.06.024>.
- [3] Ricciardi TR, Petrou K, Franco JF, Ochoa LF. Defining customer export limits in PV-rich low voltage networks. *IEEE Trans Power Syst* 2019;34:87–97. <http://dx.doi.org/10.1109/TPWRS.2018.2853740>.
- [4] von Appen J, Stetz T, Braun M, Schmiegel A. Local voltage control strategies for PV storage systems in distribution grids. *IEEE Trans Smart Grid* 2014;5:1002–9. <http://dx.doi.org/10.1109/TSG.2013.2291116>.
- [5] Azim MI, Tushar W, Saha TK. Regulated P2P energy trading: A typical Australian distribution network case study. In: 2020 IEEE Power & Energy Society General Meeting. 2020, p. 1–5. <http://dx.doi.org/10.1109/PESGM41954.2020.9282128>.
- [6] Energex. Connections. Available at: <https://www.energex.com.au>.
- [7] Liu M, Ochoa L. Deliverable 1.1: Operating envelopes calculation architecture. University of Melbourne (Project EDGE); 2021, Available at: <https://electrical.eng.unimelb.edu.au/power-energy/projects/project-edge>.
- [8] Iria J, Scott P, Attarha A, Soares F. Comparison of network-(in) secure bidding strategies to coordinate distributed energy resources in distribution networks. *Sustain Energy Grids Netw* 2023;36:101209. <http://dx.doi.org/10.1016/j.segan.2023.101209>.
- [9] Blackhall L. On the calculation and use of dynamic operating envelopes evolve project M4 knowledge sharing report. Technical report, The Australian National University; 2020, Available at: <https://arena.gov.au/assets/2020/09/on-the-calculation-and-use-of-dynamic-operating-envelopes.pdf>.
- [10] Alam MR, Nguyen PT, Naranpanawe L, Saha TK, Lanckshwara G. Allocation of dynamic operating envelopes in distribution networks: Technical and equitable perspectives. *IEEE Trans Sustain Energy* 2024;15:173–86. <http://dx.doi.org/10.1109/TSTE.2023.3275082>.
- [11] Gerdroodbari YZ, Khorasany M, Razzaghi R. Dynamic PQ operating envelopes for prosumers in distribution networks. *Appl Energy* 2022;325:119757. <http://dx.doi.org/10.1016/j.apenergy.2022.119757>.
- [12] Petrou K, Procopiou AT, Gutierrez-Lagos L, Liu MZ, Ochoa LF, Langstaff T, et al. Ensuring distribution network integrity using dynamic operating limits for prosumers. *IEEE Trans Smart Grid* 2021;12:3877–88. <http://dx.doi.org/10.1109/TSG.2021.3081371>.
- [13] Liu M, Ochoa LF, Ting T, Theunissen JDJ. Bottom-up services & network integrity: The need for operating envelopes. In: CIRED 2021 - The 26th International Conference and Exhibition on Electricity Distribution. 2021, p. 1944–8. <http://dx.doi.org/10.1049/icp.2021.2117>.
- [14] Liu MZ, Ochoa LF, Wong PK, Theunissen J. Using OPF-based operating envelopes to facilitate residential DER services. *IEEE Trans Smart Grid* 2022;13:4494–504. <http://dx.doi.org/10.1109/TSG.2022.3188927>.
- [15] Mahmoodi M, Blackhall L, Noori R. A. SM, Attarha A, Weise B, Bhardwaj A. DER capacity assessment of active distribution systems using dynamic operating envelopes. *IEEE Trans Smart Grid* 2024;15(2):1778–91. <http://dx.doi.org/10.1109/TSG.2023.3313550>.
- [16] Liu B, Braslavsky JH. Robust dynamic operating envelopes for DER integration in unbalanced distribution networks. *IEEE Trans Power Syst* 2022;39:3921–36. <http://dx.doi.org/10.1109/TPWRS.2023.3308104>.
- [17] Milford T, Krause O. Managing DER in distribution networks using state estimation & dynamic operating envelopes. In: 2021 IEEE PES Innovative Smart Grid Technologies - Asia. 2021, p. 1–5. <http://dx.doi.org/10.1109/ISGTAsia49270.2021.9715663>.
- [18] Hashmi MU, Hertem D. Robust dynamic operating envelopes for flexibility operation using only local voltage measurement. In: 2023 International Conference on Smart Energy Systems and Technologies. 2023, p. 1–6. <http://dx.doi.org/10.1109/SEST57387.2023.10257504>.
- [19] Liu B, Braslavsky JH, Mahdavi N. Linear OPF-based robust dynamic operating envelopes with uncertainties in unbalanced distribution networks. *J Mod Power Syst Clean Energy* 2023. <http://dx.doi.org/10.35833/MPCE.2023.000653>.
- [20] Petrou K, Liu MZ, Procopiou AT, Ochoa LF, Theunissen J, Harding J. Operating envelopes for prosumers in LV networks: A weighted proportional fairness approach. In: 2020 IEEE PES Innovative Smart Grid Technologies Europe. 2020, p. 579–83. <http://dx.doi.org/10.1109/ISGT-Europe47291.2020.9248975>.
- [21] Attarha A, SMNR, Scott P, Thiébaux S. Network-secure envelopes enabling reliable DER bidding in energy and reserve markets. *IEEE Trans Smart Grid* 2022;13:2050–62. <http://dx.doi.org/10.1109/TSG.2021.3138099>.
- [22] Verzijlbergh RA, De Vries LJ, Lukszo Z. Renewable energy sources and responsive demand. Do we need congestion management in the distribution grid? *IEEE Trans Power Syst* 2014;29(5):2119–28. <http://dx.doi.org/10.1109/TPWRS.2014.2300941>.
- [23] Sundstroem O, Binding C. Flexible charging optimization for electric vehicles considering distribution grid constraints. *IEEE Trans Smart Grid* 2012;3:26–37. <http://dx.doi.org/10.1109/TSG.2011.2168431>.
- [24] Massachusetts Institute of Technology (MIT). Utility of the future. 2016, Available at: <https://energy.mit.edu/wp-content/uploads/2016/12/Utility-of-the-Future-Full-Report.pdf>.
- [25] Borenstein S, Jaske MR, Rosenfeld AH. Dynamic pricing, advanced metering, and demand response in electricity markets. UC Berkeley: Center for the Study of Energy Markets; 2002.
- [26] Meng F, Chowdhury BH. Economics of grid-tied customer-owned photovoltaic power generation. In: 2012 IEEE Power and Energy Society General Meeting. 2012, p. 1–5. <http://dx.doi.org/10.1109/PESGM.2012.6344709>.
- [27] Sotkiewicz PM, Vignolo JM. Nodal pricing for distribution networks: Efficient pricing for efficiency enhancing DG. *IEEE Trans Power Syst* 2006;21:1013–4. <http://dx.doi.org/10.1109/TPWRS.2006.873006>.
- [28] Li R, Wu Q, Oren SS. Distribution locational marginal pricing for optimal electric vehicle charging management. *IEEE Trans Power Syst* 2014;29:203–11. <http://dx.doi.org/10.1109/TPWRS.2013.2278952>.
- [29] Huang S, Wu Q, Oren SS, Li R, Liu Z. Distribution locational marginal pricing through quadratic programming for congestion management in distribution networks. *IEEE Trans Power Syst* 2015;30:2170–8. <http://dx.doi.org/10.1109/TPWRS.2014.2359977>.
- [30] Zhao J, Wang Y, Song G, Li P, Wang C, Wu J. Congestion management method of low-voltage active distribution networks based on distribution locational marginal price. *IEEE Access* 2019;7:32240–55. <http://dx.doi.org/10.1109/ACCESS.2019.2903210>.
- [31] Singh R, Goswami SK. Optimum allocation of distributed generations based on nodal pricing for profit, loss reduction, and voltage improvement including voltage rise issue. *Int J Electr Power Energy Syst* 2010;32:637–44. <http://dx.doi.org/10.1016/j.ijepes.2009.11.021>.
- [32] Bai L, Wang J, Wang C, Chen C, Li F. Distribution locational marginal pricing (DLMP) for congestion management and voltage support. *IEEE Trans Power Syst* 2018;33:4061–73. <http://dx.doi.org/10.1109/TPWRS.2017.2767632>.
- [33] Mieth R, Dvorkin Y. Distribution electricity pricing under uncertainty. *IEEE Trans Power Syst* 2020;35:2325–38. <http://dx.doi.org/10.1109/TPWRS.2019.2954971>.
- [34] Yuan H, Li F, Wei Y, Zhu J. Novel linearized power flow and linearized OPF models for active distribution networks with application in distribution LMP. *IEEE Trans Smart Grid* 2016;9(1):438–48. <http://dx.doi.org/10.1109/TSG.2016.2594814>.
- [35] Frías P, Gómez T, Rivier J. Regulation of distribution system operators with high penetration of distributed generation. In: 2007 IEEE Lausanne PowerTech. 2007, p. 579–84. <http://dx.doi.org/10.1109/PCT.2007.4538381>.
- [36] Lanckshwara G, Sharma R, Alam MR, Yan R, Saha T. Development and validation of a dynamic operating envelopes-enabled demand response scheme in low-voltage distribution networks. 2023, ArXiv:2311.15514.
- [37] Antić T, Geth F, Capuder T. The importance of technical distribution network limits in dynamic operating envelopes. In: 2023 IEEE Belgrade PowerTech. 2023, p. 1–6. <http://dx.doi.org/10.1109/PowerTech55446.2023.10202795>.
- [38] Weckx S, D'hulst R, Driesen J. Locational pricing to mitigate voltage problems caused by high PV penetration. *Energies* 2015;8:4607–28. <http://dx.doi.org/10.3390/en8054607>.
- [39] Synergrid. Specific technical prescriptions regarding power-generating plants operating in parallel to the distribution network. 2019, Available at: <https://www.sibelga.be/asset/file/6fdacf28-619b-11ec-937e-005056970ffd>.
- [40] Girigoudar K, Roald LA. Linearized three-phase optimal power flow models for distribution grids with voltage unbalance. In: 2021 60th IEEE Conference on Decision and Control. 2021, p. 4214–21. <http://dx.doi.org/10.1109/CDC45484.2021.9683780>.
- [41] Fobes DM, Claeys S, Geth F, Coffrin C. Powermodelsdistribution.jl: An open-source framework for exploring distribution power flow formulations. *Electr Power Syst Res* 2020;189:106664. <http://dx.doi.org/10.1016/j.ejrs.2020.106664>.
- [42] Poncelet K. long-term energy-system optimization models capturing the challenges of integrating intermittent renewable energy sources and assessing the suitability for descriptive scenario analyses [Ph.D. thesis], KU Leuven; 2018.
- [43] Poncelet K, Höschle H, Delarue E, Virag A, D'haeseleer W. Selecting representative days for capturing the implications of integrating intermittent renewables in generation expansion planning problems. *IEEE Trans Power Syst* 2017;32:1936–48. <http://dx.doi.org/10.1109/TPWRS.2016.2596803>.
- [44] Gonzato S. Representativeperiodsfinder.jl. 2023, Available at: <https://gitlab.kuleuven.be/UCM/representativedaysfinder.jl>.
- [45] Clymans W, Vermeiren K, Vanden Boer D, Frank M-H, Godon L, Schils A, et al. BREGILAB WP3 RES generation: Wind & PV deployment evolution and availability factor. Technical report, VITO and Imec/EV and RMI; 2022, Available at: https://energyville.be/wp-content/uploads/2022/12/BREGILAB_WP3_RESGeneration_Methodology_final.pdf.
- [46] Baetens R, Saelens D. Modelling uncertainty in district energy simulations by stochastic residential occupant behaviour. *J Build Perform Simul* 2016;9(4):431–47. <http://dx.doi.org/10.1080/19401493.2015.1070203>.
- [47] Elia. Load and Load Forecasts, Available at: <https://www.elia.be/en/grid-data/load-and-load-forecasts>.
- [48] Wilkin B. National survey report of PV power applications in Belgium 2018. Technical report, International Energy Agency Photovoltaic Power Systems Programme (IEA PVPS); 2019, Available at: https://iea-pvps.org/national_survey/national-survey-report-of-pv-power-applications-in-belgium-2018/.
- [49] Ralon P, Taylor M, Ilas A, Diaz-Bone H, Kaires K. Electricity storage and renewables: Costs and markets to 2030. Technical report, International Renewable Energy Agency (IEA); 2017, Available at: https://www.irena.org/-/media/Files/IRENA/Agency/Publication/2017/Oct/IRENA_Electricity_Storage_Costs_2017.pdf.

- [50] Yu HJJ. A prospective economic assessment of residential PV self-consumption with batteries and its systemic effects: The French case in 2030. *Energy Policy* 2018;113:673–87. <http://dx.doi.org/10.1016/j.enpol.2017.11.005>.
- [51] European Central Bank, . Euro Foreign Exchange Reference Rates, Available at: https://www.ecb.europa.eu/stats/policy_and_exchange_rates/euro_reference_exchange_rates/html/eurofxref-graph-usd.en.html.
- [52] Masson G, Kaizuka I. Trends in photovoltaic applications 2020. Technical report, International Energy Agency Photovoltaic Power Systems Programme (IEA PVPS); 2021, Available at: https://iea-pvps.org/trends_reports/trends-in-pv-applications-2020/.
- [53] Hoppmann J, Volland J, Schmidt TS, Hoffmann VH. The economic viability of battery storage for residential solar photovoltaic systems – a review and a simulation model. *Renew Sustain Energy Rev* 2014;39:1101–18. <http://dx.doi.org/10.1016/j.rser.2014.07.068>.
- [54] Höschle H, Cadre HL, Smeers Y, Papavasiliou A, Belmans RJM. An ADMM-based method for computing risk-averse equilibrium in capacity markets. *IEEE Trans Power Syst* 2018;33:4819–30. <http://dx.doi.org/10.1109/TPWRS.2018.2807738>.
- [55] Wolgast T, Ferenz S, Nieße A. Reactive power markets: A review. *IEEE Access* 2022;10:28397–410. <http://dx.doi.org/10.1109/ACCESS.2022.3141235>.
- [56] Koirala A, Suárez-Ramón L, Mohamed B, Arbolea P. Non-synthetic European low voltage test system. *Int J Electr Power Energy Syst* 2020;118:105712. <http://dx.doi.org/10.1016/j.ijepes.2019.105712>.
- [57] Govaerts N. Distribution grid tariff design-analysis of the economic efficiency of tariff structures and forward-looking cost models [Ph.D. thesis], KU Leuven; 2022.
- [58] Elshurafa AM, Albardi SR, Bigerna S, Bollino CA. Estimating the learning curve of solar PV balance-of-system for over 20 countries: Implications and policy recommendations. *J Clean Prod* 2018;196:122–34. <http://dx.doi.org/10.1016/j.jclepro.2018.06.016>.
- [59] International Energy Agency (IEA). Solar PV Power Capacity in the Net Zero Scenario, 2015–2030, Available at: <https://www.iea.org/data-and-statistics/charts/solar-pv-power-capacity-in-the-net-zero-scenario-2015-2030>.
- [60] Bezanson J, Edelman A, Karpinski S, Shah VB. Julia: A fresh approach to numerical computing. *SIAM Rev* 2017;59(1):65–98. <http://dx.doi.org/10.1137/141000671>.
- [61] Dunning I, Huchette J, Lubin M. JuMP: A modeling language for mathematical optimization. *SIAM Rev* 2015;59:295–320. <http://dx.doi.org/10.1137/15M1020575>.
- [62] Gurobi Optimization, LLC. Gurobi optimizer reference manual. 2023, URL <https://www.gurobi.com>.
- [63] Wächter A, Biegler LT. On the implementation of an interior-point filter line-search algorithm for large-scale nonlinear programming. *Math Program* 2006;106:25–57. <http://dx.doi.org/10.1007/s10107-004-0559-y>.